

Ocean Acidification Effects on Photosynthesis in Tropical Marine Macroalgae

by

Regina C Zweng

A Thesis Submitted to the Faculty of

The Charles E. Schmidt College of Science

In Partial Fulfillment of the Requirements for the Degree of

Master of Science

Florida Atlantic University

Boca Raton, FL

May 2017

Copyright by Regina Zweng 2017


Ocean Acidification Effects on Photosynthesis in Tropical Marine Macroalgae


by


Regina C Zweng

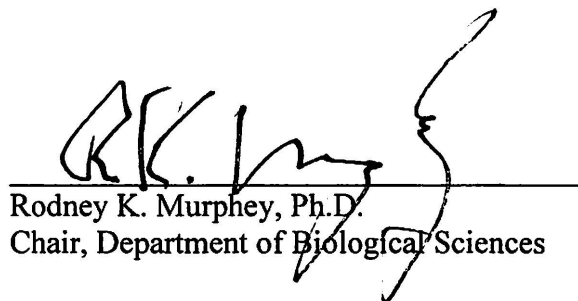
This thesis was prepared under the direction of the candidate's thesis advisor, Dr. Marguerite Koch, Department of Biological Sciences, and has been approved by the members of her supervisory committee. It was submitted to the faculty of the Charles E. Schmidt College of Science and was accepted in partial fulfillment of the requirements for the degree of Master of Science.


SUPERVISORY COMMITTEE:


Marguerite Koch
Thesis Advisor, Ph.D.


Brian Benscoter, Ph.D.


Xing-Hai Zhang, Ph.D.


Rodney K. Murphey, Ph.D.
Chair, Department of Biological Sciences


Ata Sarajedini, Ph.D.
Dean, Charles E. Schmidt College of Science


Deborah L. Floyd, Ed.D.
Dean, Graduate College

May 12, 2017
Date

Acknowledgements

I appreciate the guidance from my advisor Dr. Marguerite Koch, committee members Dr. Xing-Hai Zhang and Dr. Brian Benscoter, and Dr. George Bowes who provided valuable insight that helped guide the research and critical feedback on my thesis. I thank all my fellow lab members Kate Peach, Conall McNicholl, Christopher Johnson, Theresa Strasizar and Kim McFarlane for field and lab support as well as advice on experimental design. I appreciate the help of undergraduate student researchers, particularly Arielle Mitchell. I thank the Central Caribbean Marine Institute (CCMI) Little Cayman Research Institute staff, especially Dr. Carrie Manfrino for logistical and field support in the Cayman Islands. I am grateful for funding provided by the National Science Foundation through Grant # 140-381 for supporting this research.

Abstract

Author: Regina Zweng
Title: **Ocean Acidification Effects on Photosynthesis in Tropical Marine Macroalgae**
Institution: Florida Atlantic University
Thesis Advisor: Dr. Marguerite Koch
Degree: Master of Science
Year: 2017

Field data from CO₂ vents, a current model of future ocean acidification conditions, show a positive correlation between elevated seawater *p*CO₂ and fleshy macroalgal abundance, as well as a negative correlation between elevated seawater *p*CO₂ and calcareous macroalgal abundance on coral reefs. One underlying physiological mechanism for increases of fleshy macroalgae species in response to greater *p*CO₂ could be an increase in their photosynthesis. Furthermore, inorganic carbon use mechanisms, irradiance and depth may influence species-specific responses to ocean acidification. Therefore, this thesis aimed to discern carbon use strategies and photosynthetic responses to elevated *p*CO₂ of dominant tropical fleshy and calcareous macroalgae. All species studied were able to utilize HCO₃⁻ for photosynthesis. 33% of calcifying macroalgae and 80% of fleshy macroalgae had increased photosynthetic rates in response to lower pH. Thus, future conditions of OA may perpetuate or exacerbate the abundance of fleshy seaweeds at the expense of calcareous species.

Ocean Acidification Effects on Photosynthesis in Tropical Marine Macroalgae

Chapter 1 –Calcifying or fleshy form, C-use strategy and phyla effects on photosynthetic responses to ocean acidification in tropical macroalgae	1
Abstract.....	1
Introduction	2
Methods	5
Species and Sampling Sites	5
pH Experiment	6
Inhibitor Experiments	8
pH and AZ Interaction Experiments	9
Isotope Analysis.....	9
Statistical Analyses	10
Results	11
Seawater parameters	11
pH Experiments	11
Inhibitor experiments	12
pH and AZ Interaction Experiments	13
$\delta^{13}\text{C}$ Isotopes.....	13
Discussion.....	13
Chapter 2 - The role of C-use strategy, irradiance and depth in determining photophysiological responses of reef macroalgae to ocean acidification.....	20

Abstract.....	20
Introduction	21
Methods	26
L. variegata and Peyssonnelia sp. Experiments	26
Dominant Reef Macroalgae pH Experiment.....	29
Species and Sampling Sites	30
Isotope Analysis.....	31
Statistical Analyses	31
Results	32
L. variegata and Peyssonnelia sp. Experiments	32
Dominant Macroalgae pH Experiment	33
Isotope Analysis.....	34
Discussion.....	34
Appendices.....	43
Appendix 1 – Tables.....	44
Appendix 2 – Figures	62
References.....	75

Chapter 1 –Photosynthetic responses to ocean acidification in tropical macroalgae

Abstract

There is recent evidence showing that lowered pH and increased $p\text{CO}_2$ correlates with increases of macroalgal growth and percent cover. One underlying physiological mechanism could be an increase in photosynthetic rates in response to greater $p\text{CO}_2$. Photosynthetic responses may depend on species specific carbon use mechanisms by differentiating which species are carbon limited under current conditions. This study determined the photosynthetic response of five calcifying and three fleshy tropical macroalgal species to increases in $p\text{CO}_2$ and decreases in pH. Additionally, carbon-use strategies determined by using inhibitors of external carbonic anhydrase (CA_{ext}), anion-exchange (AE) proteins, plasmalemma (P) -type ATP-ase H^+ pumps, and acidification of the seawater at the thalli surface. The role of pH on CA_{ext} activity for two species and $\delta^{13}\text{C}$ isotope signatures were determined for all eight species. 75% of species studied increased photosynthesis by 14-46% at pH levels (7.8) predicted for the year 2100. Overall, brown fleshy and green calcifying species had greater increases than red calcifying species. Additionally, all species studied used HCO_3^- primarily via CA_{ext} . The use of HCO_3^- mediated by CA_{ext} accounted for 50-110% of net photosynthesis. Even across a range of pH, CA_{ext} mediated HCO_3^- was used for photosynthesis in *Canistrocarpus cervicornis* and *J. adhaerens* ($p=6.91\text{e-}07^*$, $3.2\text{e-}05^*$). This study also offers the first evidence for P-type ATP-ase H^+ pumps and

AE proteins in tropical red macroalgae indicating a broad array of carbon use mechanisms are available for tropical species to use HCO_3^- to reduce carbon limitation under current ocean pH. Previously, these strategies had only been found in temperate macroalgae or microalgae. This study indicates that though many tropical species use HCO_3^- at current ocean pH (8.1), they have the capacity to increase photosynthesis in response to elevated $p\text{CO}_2$ potentially shifting to greater CO_2 use under ocean acidification.

Introduction

The oceans currently absorb 30% of anthropogenic CO_2 emissions annually and this CO_2 load since the industrial revolution has lowered ocean pH globally by 0.1 units changing ocean chemistry (Feely et al 2004, Caldeira and Wickett 2003). Ocean chemical changes include reduction of pH and $[\text{CO}_3^{2-}]$, and increases of $[\text{CO}_2]$, $[\text{H}^+]$ and $[\text{HCO}_3^-]$ (Feely et al 2004). These chemical shifts, termed ocean acidification are likely to have wide-ranging impacts on marine organisms that are sensitive to shifts in carbonate chemistry with potential negative cascading effects on marine ecosystems (Doney et al 2009). With increases in CO_2 and HCO_3^- ocean acidification has the potential to affect algal photosynthesis when carbon is limiting (Hurd et al 2011). A review of ocean acidification studies indicate that raising ocean CO_2 and lowering pH may have a negative effect on growth, calcification and metabolism of many calcifying macroalgae, and a positive effect on growth of non-calcareous, fleshy macroalgae (Kroeker et al 2010, Kroeker et al 2013). However, the mechanisms accounting for these physiological and growth responses for different macroalgal species are elusive and may be driven by

species-specific photophysiology, phyla (genetic similarity), or functional form (calcareous vs fleshy).

Inorganic carbon uptake strategies may be a factor in determining macroalgal responses to elevated $p\text{CO}_2$, because individual species utilize various mechanisms of inorganic carbon uptake. Many marine macroalgae depend on HCO_3^- to supplement CO_2 as a source of inorganic carbon for photosynthesis. This is due to the fact that ocean pH maintains CO_2 concentrations in seawater at extremely low values ($14 \mu\text{M}$) compared to HCO_3^- ($2200 \mu\text{M}$) and slow diffusion rates of gases in water (10,000 times lower) than air result in CO_2 limitation (Hurd 2009). To overcome this limitation, many macroalgae use mechanisms to take advantage of the high concentration of HCO_3^- (Raven et al 1997, 2011). One common mechanism employed by 95% of macroalgae, primarily temperate macroalgal species, is the use of external carbonic anhydrase (CA_{ext}) to catalyse the dehydration of HCO_3^- to CO_2 externally which can subsequently enter the cell through passive diffusion (Haglund et al 1992, Mercado et al 1997, Koch et al 2013). A second, less common mechanism is the use of P-type ATP-ase H^+ pumps that lower the pH at the algal surface and shift the carbonate equilibria towards CO_2 . They can also generate a proton motive force used in active transport of CO_2 or HCO_3^- (Kübler et al 1999, Klenell et al 2002, Giordano et al 2005). So far, evidence for H^+ pumps has been presented for only a few green and brown temperate marine macroalgal species and tropical and temperate microalgae (Mercado et al 2006). Another less common mechanism found in Ulvophyte algae, and some Phaeophytes is an anion exchange (AE) protein that facilitates the active uptake of HCO_3^- (Drechsler et al 1993; Larsson et al 1997; Larsson and Axelsson 1999; Fernandez et al 2014). Due to the fact that species using HCO_3^- may

be less carbon limited under today's $p\text{CO}_2$ levels than species that rely solely on CO_2 , it has been hypothesized that algae which use HCO_3^- will be less responsive to increases in $p\text{CO}_2$, than species that only use CO_2 (Kroeker et al 2010). This is supported by studies that show species of algae that rely exclusively on CO_2 have increased growth and photosynthesis when grown in elevated $p\text{CO}_2$ (Kübler 1999). Other studies have found macroalgae that utilize HCO_3^- elicit no photosynthetic response to elevated $p\text{CO}_2$. Therefore, determining species-specific carbon use strategies can ascertain the role of carbon use strategies in determining carbon limitation and therefore assist in predicting which species will respond positively to elevated $p\text{CO}_2$ under continued acidification of the oceans.

A second factor that may influence how a species responds to elevated CO_2 is its phylum and functional form. Macroalgae are classified into three phyla: Rhodophyta, Phaeophyta, and Chlorophyta. 80% of brown macroalgal species reviewed from previous studies had increased photosynthetic rates at lower pH and elevated $p\text{CO}_2$. In contrast, only 18% of red species and 23% of green species showed a positive effect. When differentiating between calcified and noncalcareous macroalgae, only 17% of calcified species reviewed showed a positive response to OA, whereas 63% of noncalcareous species had a positive response. Determining differences in photosynthetic responses between calcifying and fleshy species will be important because differential responses can have cascading effects on ecosystem functioning given that calcifying and fleshy algae can co-exist and play different ecological roles.

Thus, this study examined the role of species carbon use strategy, phyla and calcified vs. fleshy form in determining tropical macroalgal species' photosynthetic

responses across a range of pH and increased $p\text{CO}_2$, including conditions predicted for 2100 scenarios (RCP 8.5, IPCC 2013). I hypothesized that photosynthesis would increase in response to lowered pH and elevated $p\text{CO}_2$ in species solely dependent on CO_2 , and without the capacity to utilize HCO_3^- , for photosynthesis. The majority of tropical macroalgae, similar to temperate species, are predicted to utilize CA_{ext} for dehydration of HCO_3^- . I also predict that tropical macroalgae would have limited capability to utilize active AE protein HCO_3^- transporters, proton pumps and boundary layer acidification to sequester inorganic carbon consistent with temperate species. Macroalgal responses are likely to be phyla-specific with greater responses in brown compared to red and green species based on the dominance of the brown phyla at CO_2 enriched field sites. To examine these hypotheses, I determined photosynthetic rates across a range of irradiances and pH levels for three fleshy and five calcifying tropical macroalgal species from the Florida Reef Tract.

Methods

Species and Sampling Sites

Approximately 100 individuals of five calcifying and three fleshy macroalgae species were collected from a shallow (~3 m) patch reef site along the Florida Reef Tract at Looe Key (24° 37.233' N, 81° 22.247' W, Fig. 1.1) on five collection trips from May 2016 to January 2017. Species included representatives from the three macroalgal phyla, Rhodophyta Chlorophyta and Phaeophyta as well as varied forms, calcified green algae (*Halimeda opuntia* and *Udotea luna*), calcified red algae (*Jania adhaerens*, *Neogoniolithon*, assemblage of crustose corraline algae (CCA)), fleshy brown algae (*Sargassum fluitans*, *Canistrocarpus cervicornis* (previously genus *Dictyota*)), and a

fleshy red alga (*Laurencia intricata*). With the exception of CCA, algae were collected by removing the whole algal thalli from the substrate selecting individuals with few or no epiphytes. CCA were collected on small Plexiglas plates (2 x 1 cm) that were attached to the substrate and allowed to settle and grow for approximately 5 mo.

During macroalgal collections, site pH (Orion A211, 8302BNUMD), temperature, light and salinity (YSI 3100) were determined in the field. Water samples (n = 3) were collected to determine total alkalinity (TA; CRM; Andrew Dickson Lab, Scripps Institute of Oceanography) within 48 h of collection using an automated titrator (Titrand® Metrohm USA, Inc.). Five carboys of seawater were collected from the site so all experiments could be run with in situ seawater. Alkalinity, temperature, conductivity (YSI 3100) and pH data were used to calculate DIC speciation (CO₂ SYS; Pierrot et al. 2006). Macroalgae were transported to the laboratory in an aerated cooler with in situ seawater and transferred to lab aquaria previously lined with carbonate sand and filled with water collected from the field site. Aquaria were kept in a 27° C water bath under a 12:12 artificial light/dark cycle (150). Salinity and temperature were measured and maintained at ambient levels (36-38 psu and 27 °C) throughout the experiment. All experiments were run within two weeks of collection.

pH Experiment

To examine the effects of *p*CO₂ and pH on macroalgal photosynthesis, photosynthetic and respiration rates were determined at four pH values: high (8.5), ambient (8.1), projected levels for 2100 (7.8 pH, RCP 8.5, IPCC 2013), and low (7.5). Experimental seawater was filtered using a 1.2 µm fiberglass prefilter and a 0.45 µm cellulose filter by vacuum filtration. To achieve pH treatments, CO₂ gas was bubbled into

seawater to lower pH (7.8 and 7.5) and 0.1 M NaOH added to raise pH (8.5). The pH meter (Orion A211, 8302BNUMD) was calibrated daily with a pH standard (Dickson Lab, Scripps Institute of Oceanography). Alkalinity measured after adjusting pH of treatment water, temperature, conductivity (YSI 3100) and pH data were used to calculate CO₂ concentrations in each pH treatment (CO₂ SYS; Pierrot et al. 2006). Alkalinity was 2369, 2378, 2449, and 2805 for treatments 7.5, 7.8, 8.1, and 8.5 respectively. The higher alkalinity in treatment 2805 was most likely due to the method of adjusting pH with NaOH (Hurd et al 2009). Before experiments, O₂ content was reduced to ~80% saturation by bubbling N₂ gas to ensure O₂ did not reach super-saturation during incubations and reduce the potential effects of photorespiration.

Photosynthesis-Irradiance (PI) curves were determined for each replicate in a O₂ electrode system (Chlorolab, Hansatech). The O₂ electrode was calibrated daily with air-saturated seawater bubbled with compressed air and deoxygenated seawater prepared by bubbling with N₂ gas into filtered (0.45µm) seawater for ~10 min. Light was provided by an LED light source (LH36/2R, Hansatech, UK) calibrated daily and programmed to increase every two minutes to eight preset, irradiance levels (0, 50, 100, 200, 400, 600, 900, 1200 µmol photon m⁻² s⁻¹). Biologically induced changes in seawater chemistry were reduced by a short incubation time of 16 min. Water temperature was controlled using a circulating water bath set to 27°C, the mean annual temperature on the Florida Reef Tract. Each replicate (n = 7-8) of 0.5 g fresh tissue mass of calcified species or 0.25 g fresh tissue mass of fleshy species was placed into the chlorolab along with filtered (0.45 µm) seawater. The amount of seawater optimal for detecting a signal was determined for each species prior to experimentation and was between 16-20 mL. O₂ flux rates were

normalized to fresh tissue mass with the exception of CCA, which was normalized to surface area. Photosynthesis-irradiance curves were calculated using a hyperbolic regression model (Jassby and Platt 1976, $P_{\text{net}} = P_{\text{max}} \times \tanh(\alpha I / P_{\text{max}}) + R$) and photosynthetic parameters were calculated using Excel's data solver tool (Lobo et al 2013). Parameters included photosynthetic efficiency (α), maximum net photosynthesis (P_{max}), maximum gross photosynthesis (P_{gmax}), light compensation point (I_c), and respiration (R).

Inhibitor Experiments

Inorganic carbon uptake mechanisms were examined for each species by measuring photosynthetic rates in the presence and absence of inhibitors that block individual mechanisms. Inhibitors included acetazolamide (AZ, Sigma Aldrich, 99.98%) which inhibits the dehydration of HCO_3^- into CO_2 by external CA (Drechsler et al 1993), Pyridoxal (5) phosphate (PLP, Fisher Scientific) which inhibits the active uptake of HCO_3^- , Tris (Trizma R preset crystals, Sigma Aldrich) that blocks acidification of the boundary layer (Mercado et al 2006) and Sodium Orthovanadate (Vanadate, Sigma Aldrich, 99.98%) which interferes with P-type ATPase proton pumps (Klenell et al 2002). Solutions of AZ (200 μM), PLP (480 μM) and Tris (50 mM) were dissolved in filtered seawater (0.45 μm) followed by pH adjustment to 8.1 (1M HCl). A 200 mM stock solution of vanadate was prepared by dissolving sodium orthovanadate in deionized water and activated using several cycles of boiling, cooling, and adjusting the pH to 10 using 1 M HCl. For each experimental replicate, vanadate stock solution was added to filtered (0.45 μm) seawater for a final concentration of 400 μM . The pH of experimental seawater was measured after adding the vanadate stock solution to ensure it did not alter

the pH of the seawater. Concentrations of each inhibitor were chosen using preliminary dose response curves based on previous studies (Drechsler et al 1993, Al-Moghrabi et al 1996, Mercado et al 2006).

Photosynthetic rates were measured by O₂ evolution in the same O₂ electrode system (Chlorolab, Hansatech) as used in the pH experiments described above. Irradiance levels (0, 50, 100, 200, 400, 600, 900, and 1200 $\mu\text{mol photon m}^{-2} \text{s}^{-1}$), incubation time, normalization to fresh tissue mass or surface area, PI curve construction and parameter determination were also as described above for pH experiments.

pH and AZ Interaction Experiments

To determine the effects of pH on photosynthesis supported by CA_{ext}, P-I curves were established across a range of pH in the presence and absence of AZ. Two species, *C. cervicornis* and *J. adhaerens*, were chosen for these experiments based on a significant CA_{ext} and pH response in preliminary studies. The pH levels and concentration of AZ were the same as in the single factor pH experiments. Photosynthetic rates were measured by O₂ evolution as in the pH and inhibitor experiments described above. Irradiance levels 0, 50, 100, 200, 400, 600, 900, and 1200 $\mu\text{mol photon m}^{-2} \text{s}^{-1}$, incubation time, normalization to fresh tissue mass, PI curve construction and parameter determination were also the same as described above.

Isotope Analysis

Fresh tissue samples (n = 5) of each species were collected at the Looe Key patch reef site. Upon returning to the lab, tissues were acidified to remove carbonates, dried at 60°C to constant weight, and ground with a mortar and pestle for analysis. Tissue carbon isotopic signatures ($\delta^{13}\text{C}$) were determined using a mass spectrometer (Thermo Electron

DeltaV Advantage) coupled with a CNS Elemental Analyzer (ConFlo II interface linked to a Carlo Erba NA 1500). All carbon isotopic results are expressed in standard delta notation relative to VPDB.

Statistical Analyses

All statistical tests were conducted using R (R Core Team 2013). Assumptions of normality of residuals and homogeneity of variance were examined using a Shapiro Wilkes and Levene's test, respectively. For parameters where assumptions were not met, data was transformed with a log or square root transformation. In the case that homogeneity of variance was not met after transformations, a non-parametric Kruskal-Wallis rank sum test was used in place of an ANOVA. If normality of residuals was not met, these data were not transformed because ANOVA is robust against violation of the normality assumption, particularly when variances are homogeneous (Zar, 2010). Each response variable (α , P_{\max} , $P_{g\max}$, I_c , and R) was tested separately for the pH and inhibitor experiments using ANOVA. A post hoc Tukey pairwise comparison test was used to determine which pH levels had significant differences in photosynthetic parameters. A post hoc Dunnett test was used for the inhibitor experiment to compare each inhibitor group to the control. For the pH x AZ experiment on *C. cervicornis* and *J. adhaerens*, separate two-way ANOVA's were used for $P_{g\max}$. Data was transformed using a square-root transformation to ensure homogeneity of variances. Isotope data were analyzed with a Kruskal Wallis test to determine if there were differences in $\delta^{13}\text{C}$ ratios between species.

Results

Seawater parameters

The average temperature and salinity across all field collection days was 28.2°C and 36.9 psu, respectively. The range of field pH measurements during collection days was 7.98 and 8.10. Alkalinity in the field averaged $2319 \pm 68 \mu\text{mol}\cdot\text{kg}^{-1}$. These data were used to calculate the DIC speciation in the field which was $7.8 \mu\text{mol CO}_2 \text{ kg}^{-1} \text{ SW}$, $1543.8 \mu\text{mol HCO}_3^- \text{ kg}^{-1} \text{ SW}$, and $256.2 \mu\text{mol CO}_3^{2-} \text{ kg}^{-1} \text{ SW}$. Light measured at the bottom (~3m) of the study site was $\sim 600\text{-}1000 \mu\text{mol photon m}^{-2} \text{ s}^{-1}$.

Speciation of inorganic carbon was calculated again based on treatment temperature and alkalinity after adjusting pH. Modification of ambient seawater pH for experiments resulted in a range of DIC concentrations for each treatment shown in Table 1.1. Based on these data, there was an order of magnitude greater CO_2 concentration in the 7.5 treatment compared to the 8.5 treatment (Table 1.1)

pH Experiments

The greatest effect of pH on photosynthetic parameters based on PI curves was on P_{max} and P_{gmax} . In general, P_{max} and P_{gmax} increased at lower pH with the exception of *N. strictum* and the assemblage of CCA. There were significant effects of pH on P_{gmax} for *J. adhaerens*, *L. intricata*, *H. opuntia*, *U. luna*, *S. fluitans*, and *C. cervicornis*, ($p < 0.05$, Tables 1.2, 1.3). However based on post hoc Tukey pairwise comparison tests, for *J. adhaerens* and *S. fluitans*, differences were only seen between the lowest (7.5) and highest (8.5) pH treatments (Table 1.2). There were also differences between species in the percentage that photosynthesis increased between ambient and lower pH levels. For example, *J. adhaerens* increased 14% for P_{gmax} between ambient pH and pH projected for

the year 2100, while *U. luna* increased 46%. There was also an inhibitory effect on photosynthesis at the highest pH (8.5) compared to ambient pH (8.1). All species with significant photosynthetic effects of pH on P_{gmax} also had significant effects of pH on P_{max} with the exception of *S. fluitans*. *Sargassum fluitans* was the only species to show a significant effect of pH on respiration ($p < 0.05$, Table 1.3). Based on Tukey post hoc comparison tests, there was 37% lower respiration at pH 8.5 than at pH 7.8, the level projected for the year 2100 (RCP 8.5 IPCC 2013). *Laurencia intricata*, *S. fluitans*, and *U. luna* also had higher photosynthetic efficiency (α) at lower pH ($p < 0.05$, Tables 1.2, 1.3, Figure 1.2) with *H. opuntia* approaching a significant difference ($p = 0.07$, Tables 1.2, 1.3 Figure 1.2). *Halimeda opuntia*, *L. intricata*, and *U. luna* also had lower irradiance compensation points at lower pH (Tables 1.2, 1.3, Figure 1.2).

Inhibitor experiments

All species with the exception of *N. strictum* had reduced P_{gmax} or P_{max} in response to inhibition of CA_{ext} with AZ (Tables 1.4, 1.5, Fig 1.3). *Jania adhaerens* and *S. fluitans* showed an 83-110% reduction in P_{max} , while *C. cervicornis* and *L. intricata* P_{max} only decreased 50% (Table 1.4, Figure 1.3). Inhibition of CA_{ext} also increased the light compensation point of *H. opuntia* (Table 1.4, Fig 1.3). Inhibition of CA_{ext} had no significant affect on R or α in any species ($p > 0.05$, Table 1.5).

Inhibiting acidification of the boundary layer with Tris buffer reduced P_{max} by approximately 50% in *L. intricata* and *S. fluitans* and nearly completely in *U. luna*. Tris also increased respiration in *L. intricata*. *Laurencia intricata* had reduced P_{max} in the presence of vanadate and PLP, which blocks an ATP-ase proton pump, and an anion-

exchange protein respectively. The only other species sensitive to PLP was *J. adhaerens* which had a reduced P_{\max} . I_c and α were unaffected by PLP and vanadate in all species.

pH and AZ Interaction Experiments

There were significant effects of pH on the inhibitory effect of AZ for both *J. adhaerens* and *C. cervicornis*. $P_{g\max}$ increased in response to lower pH for *C. cervicornis* and was lower at high pH in the presence and absence of AZ. In the absence of AZ, $P_{g\max}$ of *J. adhaerens* stayed relatively constant between low (7.8, 7.5) and ambient (8.1) pH treatments, but was reduced by 22% in the high pH treatment of 8.5. In contrast, inhibition of CA_{ext} reduced photosynthesis across all pH levels for both species (Table 1.6, Fig 1.4). There was no statistically significant pH by AZ interaction ($p > 0.05$, Table 1.6); however, there was less of an effect of AZ on $P_{g\max}$ at the lowest pH level for *J. adhaerens* (Fig. 1.4). There was only an 8% reduction of photosynthesis with inhibition of CA_{ext} at pH 7.5, but a 48% reduction at ambient pH (8.1).

$\delta^{13}\text{C}$ Isotopes

The organic tissue of all species examined fell within a relatively narrow range of -14 and -20 $\delta^{13}\text{C}$ indicative of at least partial HCO_3^- use (Fig. 1.5). While there was no significant groupings amongst algal forms (calcifiers or fleshy) or taxonomic phyla, there were statistical differences between species based on a Kruskal-Wallis test ($df=7$, $X^2=34.4$, $p=1.3\text{E}-5$).

Discussion

Based on data from the present short-term study, many tropical macroalgal species have the potential to increase photosynthesis in response to future increases of $p\text{CO}_2$, particularly at the lowest pH (7.5) and saturating irradiance. Out of the eight

species studied, 75% had increased P_{gmax} or P_{max} as a result of lower pH and higher pCO_2 . However, most species in this study, did not show different photosynthetic rates between ambient (8.1) and projected levels by the year 2100 (7.8, IPCC 2013), but differences were observed at the lowest pH value of 7.5. Although 7.5 is not the projected global mean pH, near shore coastal communities can have diel fluctuations within this range in the mornings after a night of respiration (Peach et al 2017, Cornwall et al 2013, Hoffman et al 2011, Hurd et al 2011, Price et al 2012), and values as low as 7.4 have been measured in some near shore environments (Wootton 2008). Four species had increases in α or I_c indicating that they increase photosynthetic rates at low irradiance and lower pH. These were *U. luna*, *S. fluitans*, *H. opuntia*, and *L. intricata*. In contrast, although *C. cervicornis* and *J. adhaerens* had increased P_{gmax} , there was no effect of low pH on α . This indicates that some species are able to increase photosynthesis in response to increased pCO_2 at sub-saturating light, while others may only have increased photosynthesis at saturating light. Since all species within this patch reef community were found in the same high-light environment (700-1200 $\mu\text{mol photons m}^{-2} \text{s}^{-1}$), light limitation should not constrain their response to elevated pCO_2 . However, in other situations light limitation can negate photosynthetic responses to increased pCO_2 (Celis-Plá et al 2015).

Macroalgal responses to increased pCO_2 and lower pH showed modest correlation to phyla and functional form. For example, pH had the least effect on red calcareous species photosynthesis, such as *N. strictum* and the CCA assemblage with no statistically significant differences in photosynthetic parameters between any pH treatments. The other red calcareous algae, *J. adhaerens*, had a statistically significant difference in P_{max}

and P_{gmax} at different pH levels, but based on a Tukey pairwise comparison test, it was only significant between the lowest (7.5) and highest (8.5) pH treatments. The findings of no or only modest photosynthetic responses of red calcareous algae at low pH and high pCO_2 are similar to other reports for red calcareous species (Johnson et al 2014). It is also consistent with overall trends found in the literature on the effects of elevated pCO_2 on macroalgal photosynthesis where only 23% of red coralline algae increased photosynthesis in response to elevated pCO_2 (Table 1.7).

Both upright calcareous green species, *U. luna* and *H. opuntia*, had increased P_{max} and P_{gmax} in response to elevated pCO_2 and lower pH. The results for *H. opuntia* are in contrast with others that found a neutral or negative effect of pCO_2 on photosynthesis (Hoffman et al 2014, Peach et al 2017, Price et al 2011, Johnson et al 2014, Vogel et al 2015). Differences in studies may be due to lower irradiance ranging from 436-614 $\mu\text{mol photons m}^{-2} \text{s}^{-1}$ (Johnson et al 2014) and 150 $\mu\text{mol photons m}^{-2} \text{s}^{-1}$ (Vogel et al 2015). My study indicates that saturating irradiance is necessary in some species for a positive photosynthetic response to elevated pCO_2 .

Increases in P_{gmax} were observed at lower pH for the three fleshy species studied: *C. cervicornis*, *S. fluitans*, and *L. intricata*. This is consistent with previous literature (see Table 1.7) showing that fleshy algae, especially in the brown phyla, are more likely to have increased photosynthesis in response to elevated pCO_2 . Additionally, a previous study found that *C. cervicornis* has increased potency of allelochemicals when grown under elevated pCO_2 which leads to increased competitive ability compared to corals (Del Monaco et al. 2017). The higher rates of photosynthesis under elevated pCO_2 found here may provide a physiological driver for more resources available for allelochemical

production by macroalgae. Elevated P_{gmax} of *C. cervicornis* and *S. fluitans* in response to elevated pCO_2 found in my study could also provide energy and resources that help explain their expansion in naturally acidified sites including natural CO_2 seeps. In field studies near CO_2 vents, the percent coverage of *Sargassum*, *Dictyota* and other fleshy species increased from near 0% to 60% while coralline algae decreased from >60% to 0% cover (Hall-Spencer 2008). In another field study of a naturally occurring pH gradient, *Dictyota* increased abundance at lower pH areas, while *Sargassum* was only found in the lowest pH site (Porzio et al 2011). In my study, both brown fleshy macroalgae in these genera were able to increase photosynthetic parameters in response to elevated pCO_2 offering a possible explanation for their success in low pCO_2 environments.

While the majority of the tropical macroalgae examined indicated an increase in photosynthesis under elevated pCO_2 and a lower pH, with some differences corresponding to form and phyla, the mechanisms controlling this response based on their dependence of various c-use strategies is only now being elucidated. Although algae utilizing HCO_3^- might be expected to be less likely to respond to elevated pCO_2 , the current work found that some HCO_3^- -users did respond positively to elevated pCO_2 and lower pH. The inhibitor studies demonstrate that a variety of tropical species utilize CA_{ext} , and 80% of CA_{ext} -users were able to respond positively to elevated pCO_2 . The percentage of photosynthesis inhibited by AZ ranged from 32-65% reduction of P_{gmax} for different species, which suggests that around 35 - 68% of photosynthesis is supported by passive diffusion of CO_2 . This percentage of photosynthesis attributed to passive CO_2 diffusion provides an opportunity for algae to respond to elevated pCO_2 . CA_{ext} was found across different phyla and functional groups in agreement with other studies (Maberly et

al 1992, Koch et al 2013), a portion of photosynthesis was reliant on CO₂. The current two factor experiment with pH and AZ gives insight into the role of CA_{ext} in inorganic carbon acquisition across different pH levels for *C. cervicornis* and *J. adhaerens*. The reduction of photosynthesis due to CA_{ext} inhibition was not dependent on pH treatments. Although algae still utilize CA_{ext} for a portion of photosynthesis at low pH, they were still able to increase photosynthesis at lower pH by taking advantage of increased *p*CO₂.

Tropical macroalgae appear to have the capacity to sequester inorganic carbon across a range of pH by taking advantage of a diversity of inorganic carbon use mechanisms, as well as increase diffusive uptake of CO₂ when available. These data offer some of the first evidence for anion exchange proteins and ATPase H⁺ pumps in tropical macroalgae. Evidence for an anion-exchange protein was found in *J. adhaerens* and *L. intricata*. Thus far, the evidence for anion-exchange proteins has been found in temperate brown algae such as the giant kelp *Macrocystis pyrifera* (Fernandez et al 2014) and green algae in the family Ulvophyceae (Drechsler et al 1993). Acidification of the boundary layer was also found to be important for *S. fluitans*, *L. intricata*, and *U. luna*. One possible mechanism for acidification of the boundary layer is the use of an ATP-ase H⁺ pump. However, only *L. intricata* showed evidence for an ATP-ase pump in inhibitor experiments. Therefore, *L. intricata* may be using an ATP-ase H⁺ pump while *U. luna* and *S. fluitans* are using a different mechanism to acidify the boundary layer. These results into specific carbon uptake mechanisms offer more detail than other studies, which use pH drift experiments or carbon isotope signatures that cannot distinguish between different mechanisms of HCO₃⁻ use. Further, pH drift experiments are dependent on long-term incubations where other factors may confound results. Based on inhibitor

experiments, a diversity of mechanisms in tropical macroalgae are present that allow photosynthesis to be driven by HCO_3^- when seawater pH may limit the uptake of CO_2 .

The organic tissue carbon isotope signatures also indicate widespread use of HCO_3^- for photosynthesis among dominant tropical macroalgae. Algae with $\delta^{13}\text{C}$ values between -10 and -30‰ are often classified as using both HCO_3^- and CO_2 for photosynthesis (Maberly et al. 1992; Raven et al. 2002, Diaz-Pulido 2016). All $\delta^{13}\text{C}$ values in this study fall within the lower to middle part of this range suggesting that they all use both HCO_3^- and CO_2 . The pH by AZ experiments on *C. cervicornis* and *J. adhaerens* lead to the suggestion that algae use CA_{ext} facilitated HCO_3^- and CO_2 across a range of pH conditions as there was no significant interaction term ($p > 0.05$, Table 1.6). The carbon isotope signature of *N. strictum* indicated HCO_3^- use; however, it was unaffected by all of the inhibitors examined (Table 1.5, Figure 1.3). Therefore, this species may be using a mechanism not tested in this study. Another possibility is that as a calcifier there are different carbon use mechanisms for CO_2 sequestration related to calcification that are influencing $\delta^{13}\text{C}$ values of organic tissues (Diaz-Pulido et al 2016). The relatively narrow range of $\delta^{13}\text{C}$ values compared to other studies that looked at macroalgae in reef environments implicate the importance of environmental conditions driving inorganic carbon use. The Looe Key patch reef site has relatively high irradiance ($\sim 600\text{-}1000 \mu\text{mol photon m}^{-2} \text{s}^{-1}$) and all species were collected from the same area around the patch reefs. Research from Little Cayman Island reefs and those by Diaz-Pulido et al (2016) where macroalgae were collected along reefs from 1 – 10 m (Diaz-pulido et al 2016) and 12 - 19 m (chapter 2) $\delta^{13}\text{C}$ signatures spanned a broader range (0.5 – 33 ‰ Diaz-Pulido et al 2016). These results, and the PI curves, suggest that irradiance can

also influence the use of HCO_3^- and CO_2 , that may result in distinct $\delta^{13}\text{C}$ signatures when species are examined that come from high irradiance shallow sites compared to deep low-light environments.

Current hypotheses theorize that macroalgae with the ability to use HCO_3^- are saturated at current CO_2 levels (Giordano et al 2005) and therefore are unlikely to increase photosynthesis in response to elevated $p\text{CO}_2$ compared to species that lack CCM's (Hepburn et al 2011, Kroeker et al 2013, Cornwall et al 2012, Cornwall et al 2015, Ji et al 2016). In contrast, the results of this study indicate that macroalgal species can increase photosynthesis as $p\text{CO}_2$ increases especially in high light environments. Herein, first evidence is presented for a diversity of inorganic carbon use mechanisms, including AE proteins and ATPase H^+ pumps, that allow tropical marine macroalgae to access HCO_3^- . Many tropical macroalgae are well poised to take advantage of greater CO_2 availability with ocean acidification, but will also likely remain dependent on HCO_3^- to satisfy their carbon requirements for photosynthesis. Additional studies will be required to examine how these short-term physiological responses to elevated $p\text{CO}_2$ translate to greater growth and abundance on reef systems in the long-term.

Chapter 2 - The role of C-use mechanisms, irradiance and depth in determining photophysiological responses of reef macroalgae to ocean acidification

Abstract

There is recent evidence showing that increased $p\text{CO}_2$ and concomitant decreases in ocean pH correlate with increases of fleshy macroalgal abundance on coral reefs and decreases in crustose coralline algae (CCA). One underlying physiological mechanism for increases of fleshy macroalgae species could be an increase in photosynthesis in response to greater $p\text{CO}_2$. However, inorganic carbon use mechanisms, irradiance, and depth may influence species-specific responses to $p\text{CO}_2$ and/or OA. The predominant hypothesis in the literature suggests that species which can use HCO_3^- for photosynthesis are less carbon limited than obligate CO_2 users, and will not have increased photosynthesis in response to increased $p\text{CO}_2$. Thus, this study determined carbon use mechanisms and photosynthetic responses to increased $p\text{CO}_2$ at lower pH values of dominant fleshy and calcareous macroalgae from various depths on Little Cayman Island reefs. We used inhibitors of different carbon use mechanisms including external carbonic anhydrase, anion exchange proteins, and P-type protein pumps for the brown fleshy species *Lobophora variegata* and the CCA *Peyssonnelia sp.* We determined photosynthetic parameters for these two species across a range of irradiances at four pH values (7.5, 5.8, 8.1, and 8.5). We determined the photosynthetic rates of five other dominant macroalgal species in the genera *Halimeda* and *Dictyota* at high light and three pH levels (7.8, 8.1, and 8.5). All species were able to utilize HCO_3^- for photosynthesis,

based on $\delta^{13}\text{C}$ isotope values that ranged from -16 to -26 ‰ and correlated with depth which could be related to irradiance or CO_2 availability. *Peyssonnelia* sp. did not respond to elevated $p\text{CO}_2$, even at light saturation, compared to *L. variegata* which had a 10% increase in photosynthesis at pH 7.8 compared to 8.1 pH. Another dominant brown macroalgae on tropical reefs, *Dictyota pulchella* did not increase net photosynthesis under low pH treatments. The important sediment-producing genus *Halimeda* elicited species-specific responses: thus *H. opuntia* and *H. gorraeuii* increased photosynthesis in response to elevated $p\text{CO}_2$ by 16 and 33% respectively while *H. copiosa* and *H. tuna* showed no response. This work is the first to detect an anion exchange protein pump in a tropical red macroalgae, *Peyssonnelia* sp. It also indicates that, some HCO_3^- -users show a positive photosynthetic response with elevated $p\text{CO}_2$.

Introduction

Macroalgae are important components of coral reef ecosystems, serving the role of nutrient recycling, reef cementation, sediment production, and providing food for herbivorous fish and invertebrates (reviewed in Fong and Paul 2011). Crustose coralline algae (CCA) maintain reef structure and provide settlement cues for coral larvae (Heyward and Negri 1999, Raimondi and Morse 2000). Upright calcareous forms of algae contribute to sediment production on reefs with species of the genus *Halimeda* contributing ~8% of the global carbonate budget (Hillis 1997). Fleshy forms of macroalgae provide the base of the food web for many herbivores on reefs; however, following loss of coral cover, reefs can undergo a phase shift from a coral-dominated to a macroalgal-dominated state (Hughes 1994). Although herbivory has been well established as a controlling factor in macroalgal growth and abundance (Hughes et al.

2010), recent evidence suggests ocean acidification (OA) may also be a contributing factor (Fabricius et al. 2011; Johnson et al 2014; Enochs et al. 2015). Ocean acidification is the alteration of seawater chemistry due to the absorption of 30% of anthropogenic CO₂ emissions (Sabine et al 2004). Ocean absorption of CO₂ reduces pH, carbonate ion concentration (CO₃²⁻) and CaCO₃ saturation state, while increasing CO₂ and bicarbonate ions (HCO₃⁻)(Feely et al 2004). This shift in the carbonate equilibria can enhance fleshy macroalgal growth (Johnson et al. 2014), increase their competitive dominance over corals (Diaz-Pulido et al. 2011) and result in a high abundance of fleshy macroalgae on naturally-acidified reefs (Fabricius et al. 2011; Enochs et al. 2015). In contrast, CCA tend to have decreased growth rates in response to increased *p*CO₂ (James et al 2014). One possible physiological driver for positive fleshy macroalgal responses to OA could be an increase in photosynthesis due to additional CO₂ when inorganic carbon is otherwise limiting. However, there is conflicting evidence for photosynthetic changes in marine macroalgae in response to OA and elevated *p*CO₂ and little is known about the carbon uptake mechanisms of tropical reef macroalgae (Koch et al 2013).

Different carbon uptake mechanisms could result in species-specific responses to elevated CO₂ availability, and discriminate against species that are not inorganic carbon limited. Although all species take up CO₂ through passive diffusion, most marine macroalgae can also utilize HCO₃⁻ for photosynthesis. A dependency on HCO₃⁻ is related to the relatively low concentration of CO₂ (14 μM) compared to HCO₃⁻ (2,200 μM) at current ocean pH (8.1), and the slow diffusion rate of CO₂ in seawater (Hurd et al 2009). Presently, the majority (91%) of inorganic carbon is in the form of HCO₃⁻ (Doney et al 2009). Because of its abundance in seawater, many species have adapted to utilize HCO₃⁻

as a source for inorganic carbon by applying various carbon uptake and even concentrating mechanisms (CCMs) that lower, but not always eliminate, carbon limitation for photosynthesis (Raven et al 1997, 2011). One common mechanism found in approximately 95% of algal species is the use of extracellular, membrane-bound carbonic anhydrase (CA) to speed up the interconversion of HCO_3^- and CO_2 , followed by CO_2 diffusion across the plasmalemma (Haglund et al 1992, Mercado et al 1997, Koch et al 2013). The CA enzyme is a reversible reaction that is pH dependent, driving CO_2 hydration and HCO_3^- dehydration at high and low pH, respectively. A second, less common mechanism is the use of proton pumps that lower the pH in the diffusion boundary layer at the algal surface. Lowering pH at the thalli surface shifts the carbonate equilibrium toward CO_2 and away from HCO_3^- (Mercado et al 2006), providing another mechanisms to increase CO_2 at the boundary layer and enhance its diffusion across the plasma membrane. A third mechanism that may also be a true CCM is active uptake of HCO_3^- through an anion exchange protein. Thus far, this mechanism has only been demonstrated in microalgae and a few species of fleshy temperate macroalgae (Drechsler et al 1993; Larsson et al 1997; Larsson and Axelsson 1999; Fernandez et al 2014). While very little is known about carbon uptake in tropical macroalgae, determining which mechanisms are present in different species may explain some of the varying species responses to OA. For example, it has been theorized that obligate CO_2 users are more likely to be carbon limited under current conditions (Kübler et al. 1999), and therefore may increase photosynthesis under future increases in $p\text{CO}_2$. Further, CA-mediated CO_2 utilization may be enhanced under lower pH associated with elevated $p\text{CO}_2$ as dehydration of HCO_3^- is promoted (Moulin et al 2011, Koch et al. 2013).

Because of the extra energy requirements associated with C-uptake mechanisms and greater availability of CO₂ at deeper depths on reefs, varying responses of macroalgal photosynthesis to OA could be influenced by the depth and irradiance environment where the species dominate. Deeper waters typically have low irradiance and less energy available for photosynthesis, but are subject to deep-water upwelling that can be enriched in CO₂. Therefore, deeper low-light adapted species may be more likely to rely on passive CO₂ rather than energetically expensive CCMs (Kübler 1999, Hepburn et al., 2011; Raven et al., 2014, Cornwall 2015). In contrast, high irradiance, present on shallow reefs, provides energy (Hepburn et al., 2011) for the use of CCMs. A pattern of deeper species using less HCO₃⁻ than shallower species has been found in studies that characterize carbon use strategies in macroalgae along depth gradients in the Great Barrier Reef (Diaz-Pulido et al 2016). Deeper species that are more likely to be obligate CO₂ users may have increased photosynthetic rates with future OA. In contrast, high irradiance-adapted species in shallow habitats may be more likely to use CCM's to overcome carbon limitation. Experimentation on algae from different irradiance environments is needed to determine which species may be able to increase photosynthesis with increased CO₂. Additionally, many studies are conducted only at saturating irradiance. Therefore, more experiments that include a full range of irradiances are needed to determine how responses to OA interact with light availability. In fact, while low-light species may utilize less energy-dependent mechanisms of inorganic carbon use, they may not require greater carbon to meet their photosynthetic demands.

This study aimed to determine photosynthetic responses to OA from dominant fleshy and calcareous macroalgae from various depths on Little Cayman Island reefs. The

first set of experiments focused on a fleshy brown species, *Lobophora variegata*, which has increased its distribution throughout the Caribbean over the last decade, and on many reefs is considered a “nuisance species” (e.g. Liddel and Olhurst 1984, Edmunds 2002, Mumby et al 2005). *Lobophora. Variegata* is a lobed, foliose fleshy species found across a wide range of irradiances on Little Cayman Island in shallow hard-bottom lagoons under high irradiance, as well as in low-light environments on the deep reefs and underneath shaded ledges. In the low-light environments *L. variegata* co-occurs with lobed crustose coralline algae. Thus, I also examined a dominant lobed genus, *Peyssonnelia* sp., from low-light sites on the reef where *L. variegata* also occurs. For the first experiment, *L. variegata* and *Peyssonnelia* sp. photosynthetic rates were determined across a range of pH and their specific carbon-use mechanisms (CA-use, active uptake, proton pumping) discerned across a range of irradiances and $p\text{CO}_2$ levels. Four pH levels were examined, including high (8.5), ambient (8.1), year 2100 (7.8), and low (7.5). In a second set of experiments, I tested the effects of pH and $p\text{CO}_2$ on photosynthesis and respiration for the dominant macroalgae on Little Cayman Island reefs: two dominant fleshy brown species, *L. variegata* and *Dictyota pulchella* (eg. Liddel and Olhurst 1984, Edmunds 2002, Mumby et al 2005), and four species of *Halimeda*, the most ubiquitous calcareous green genus on the reef which serves an important role of reef sediment production. The *Halimeda* species encompassed a range of low- and high-irradiance adapted species (Peach et al 2017). I also determined the carbon isotope signature of all species’ organic tissues, to ascertain the dominant carbon-use strategies they employ in the field (Maberly et al 1992, Raven et al 2002).

I hypothesized that *L. variegata* would have the potential to respond to elevated $p\text{CO}_2$ characteristic of brown fleshy algae at low pH across a range of irradiances. Further, this species was predicted to utilize CA and other mechanisms to sustain high photosynthetic rates at saturating irradiance. In contrast, *Peyssonnelia* sp. would only respond to elevated $p\text{CO}_2$ and lowered pH through passive diffusion and lack high-irradiance dependent systems. These two species differences in C-use would result in a significantly lower $\delta^{13}\text{C}$ for *Peyssonnelia* sp. than *L. variegata*, as *L. variegata* would be able to utilize CO_2 via passive diffusion and enhanced dehydrogenated HCO_3^- , while *Peyssonnelia* sp. would be restricted to CO_2 use by diffusion. Based on a comparison of the dominant reef macroalgae on Little Cayman reefs, I proposed that the macroalgae from high-irradiance environments (*Halimeda tuna*, and *Dictyota pulchella*, *L. variegata*) would sustain high photosynthetic rates at high pH, due to their ability to engage mechanisms to supplement CO_2 uptake, although photosynthesis could be enhanced due to greater dehydrogenation of HCO_3^- at low pH. Low-light adapted species (*Peyssonnelia*, *H. Gorreauii*, *H. opuntia* and *H copiosa*) would exhibit significant increases in photosynthesis with greater CO_2 diffusion under low pH (elevated $p\text{CO}_2$) relative to high pH conditions. In general, deeper species would have lower $\delta^{13}\text{C}$ than species found in high-irradiance environments due to a greater dependence on CO_2 with less energy for CCM's and greater availability of CO_2 .

Methods

***L. variegata* and *Peyssonnelia* sp. Experiments**

pH Experiment

To examine the effects of increased $p\text{CO}_2$ on photosynthesis, net photosynthesis and respiration rates of *L. variegata* and *Peyssonnelia* sp. were determined at four pH

levels. The pH treatments were high (8.5 pH), ambient (8.1 pH), levels projected by the year 2100 (7.8 pH, RCP 8.5, IPCC 2013), and low (7.5 pH). Experimental seawater was collected from offshore reefs and filtered using a 1.2 μm fiberglass prefilter and a 0.45 μm cellulose filter by vacuum filtration. Treatment pH levels were adjusted with CO_2 gas for lower than ambient pH treatments (7.8 and 7.5) and titrated with 0.1 M NaOH for the high pH treatment (8.5). pH was measured (Orion A211, 8302BNUMD) and calibrated daily with a seawater Tris buffer (Dickson Lab, Scripps Institute of Oceanography). Alkalinity, temperature, conductivity (YSI 3100) and pH data were used to calculate CO_2 concentrations in pH treatments (CO2SYS; Pierrot et al. 2006). Total alkalinity of seawater was determined with titrations of three replicate samples using an automated titrator (Titrand® Metrohm USA, Inc.) and alkalinity reference materials (CRM; Andrew Dickson Lab, Scripps Institute of Oceanography). To reduce the influence of O_2 coming out of solution and effects of photorespiration, O_2 content was reduced in experimental seawater to ~80% saturation by bubbling N_2 gas.

Photosynthesis-Irradiance (PI) curves were determined for each replicate by O_2 evolution in a highly sensitive O_2 -electrode system (Chlorolab, Hansatech). The O_2 electrode was calibrated daily with air-saturated and deoxygenated seawater. Deoxygenated seawater was prepared by bubbling compressed N_2 gas into filtered (0.45 μm) seawater for ~10 min. Air-saturated seawater was prepared by bubbling air into filtered (0.45 μm) seawater for ~10 min. An LED light source (LH36/2R, Hansatech, UK) was calibrated daily and programmed to increase every two minutes to eight preset, irradiance levels (0, 50, 100, 200, 400, 600, 900, 1200 $\mu\text{mol photon m}^{-2} \text{s}^{-1}$). The short incubation time of 16 min minimized biologically induced changes in seawater chemistry

during the experiment. Water temperature was controlled using a circulating water bath at 27° C, the mean annual temperature at the collection sites. Each replicate (n = 4-6) of 0.5 g fresh tissue mass of *Peyssonnelia* sp. or 0.25 g fresh tissue mass of *L. variegata* was placed into the chlorolab along with 20 mL of filtered (0.45 µm) seawater. O₂ flux rates were normalized to fresh tissue mass. Photosynthesis-irradiance (PI) curves were calculated using a hyperbolic regression model (Jassby and Platt 1976, $P_{\text{net}} = P_{\text{max}} \times \tanh(\alpha I / P_{\text{max}}) + R_d$) and photosynthetic parameters were calculated using Excel's data solver tool (Lobo et al 2013). Parameters included photosynthetic efficiency (α), maximum net photosynthesis (P_{max}), maximum gross photosynthesis (P_{gmax}), light compensation point (I_c), and respiration (R).

Inhibitor Experiments

Photosynthetic rates were determined in the presence and absence of inhibitors that block individual mechanisms to determine inorganic carbon uptake mechanisms for *L. variegata* and *Peyssonnelia* sp. Acetazolamide (AZ, Sigma Aldrich, 99.98%) was used to inhibit the dehydration of HCO₃⁻ into CO₂ by external CA at the plasma membrane (Drechsler et al 1993). Pyridoxal (5) phosphate (PLP, Fisher Scientific) was used to inhibit the active uptake of HCO₃⁻. Tris (Trizma (R) preset crystals, Sigma Aldrich) was used to inhibit acidification of the boundary layer by buffering pH changes in experimental seawater (Mercado et al 2006). Sodium Orthovanadate (Vanadate, Sigma Aldrich, 99.98%) was used to inhibit P-type ATPase proton pumps (Klenell et al 2002). Solutions of AZ (200 µM), PLP (480 µM), and Tris (50 mM) were dissolved directly in filtered seawater (0.45 µm) followed by pH adjustment to 8.1 (1M HCl). A 200 mM stock solution of vanadate was prepared by dissolving sodium orthovanadate in deionized

water and activated using several cycles of boiling, cooling, and adjusting the pH to 10 using 1 M HCl. For each experimental replicate, 40 μL of vanadate stock solution was added to 20 mL filtered (0.45 μm) seawater for a final concentration of 400 μM . The pH of experimental seawater was measured after adding the vanadate stock solution to ensure it did not alter the pH of the seawater. Concentrations of each inhibitor were chosen using preliminary dose response curves and concentrations used in previous studies (Drechsler et al 1993, Al-Moghrabi et al 1996, Mercado et al 2006).

Photosynthetic rates were measured by O_2 evolution in the same O_2 -electrode system (Chlorolab, Hansatech) as was used in the pH experiments described above. Irradiance levels 0, 50, 100, 200, 400, 600, 900, and 1200 $\mu\text{mol photon m}^{-2} \text{s}^{-1}$, incubation time, normalization to fresh tissue mass, PI curve construction and parameter determination were also the same as described above for pH experiments.

Dominant Reef Macroalgae pH Experiment

Photosynthetic and respiration rates of *H. gorreauii*, *H. copiosa*, *H. opuntia*, *H. tuna*, *L. variegata*, and *D. pulchella* were measured in response to ambient pH (8.10), 2100 level pH (7.8), and high pH (8.5) treatments. Experimental seawater was collected from offshore reefs and filtered using a 1.2 μm fiberglass prefilter and a 0.45 μm cellulose filter with vacuum filtration. Adjusting pH and preparing seawater for the experiment was conducted as described above.

For each species, a small amount of wet tissue (~0.5-1 g) was added to individual tubes with 50 mL of prepared seawater ($n = 10$). The O_2 concentration was measured at the start of the experiment and the test tubes were sealed and placed in an outdoor water bath at 29°C (back reef water temperature). Light was provided by natural sunlight and

shaded with mesh screens to provide irradiances similar to those measured in the field (220-560 $\mu\text{mol photons m}^{-2} \text{s}^{-1}$). After a ~60-90 min incubation, the O_2 concentration in each replicate was measured and pH determined to ensure experimental pH levels were maintained throughout the experiment. Each replicate was covered in foil to prevent exposure to irradiance and placed back in the water bath. After a ~120 min incubation, O_2 concentration and pH were measured. The exact start and end time of each incubation were recorded for each replicate. Net photosynthesis (NPP), gross photosynthesis (GPP), and respiration (R) were calculated. Each replicate was dried, acidified with 5N HCl, and weighed. These weights were used to normalize photosynthesis and respiration rates to dry organic mass.

Species and Sampling Sites

In the Cayman Islands, the “nuisance” species of the Caribbean, *Lobophora variegata*, is wide-spread on the reefs occurring in high light environments (2.1), primarily with other fleshy species and, and in low-light environments with lobed crustose coralline algae (Fig. 2.1), such as *Peyssonnelia* sp. and low-light adapted *Halimeda* sp. (Fig. 2.1). All macroalgae thalli were collected off the north coast of Little Cayman Island from two sampling locations (Fig. 2.1), Icon Reef and Rock Bottom, using scuba. Icon reef has irradiance levels of 760 $\mu\text{mol photon m}^{-2} \text{s}^{-1}$ while Rock Bottom has irradiance levels of 50 $\mu\text{mol photon m}^{-2} \text{s}^{-1}$ in the rocky overhang where algae were collected (Peach et al 2016). *Lobophora variegata*, *D. pulchella*, and *Halimeda tuna* were collected on the tops of coral heads in ~20 m at Icon Reef. *Halimeda gorreauii*, and *H. copiosa* were collected underneath shaded ledges of the fore reef at ~24 m depth and *Peyssonnelia* sp., slightly deeper (~25 m) below the shelf edge along the wall at Rock

Bottom. *Halimeda opuntia* was collected on the sloped edge of the fore reef at ~21 m depth at Rock Bottom. Samples were kept in ambient seawater and immediately transported to the Little Cayman Island Research Center where they were placed in outdoor aquaria with seawater from the collection sites. Aquaria were exposed to natural irradiance with a mesh screen to provide irradiance levels similar to levels found on the reef (50-550 $\mu\text{mol photon m}^{-2} \text{s}^{-1}$) throughout the day. Experiments were conducted on algae within 48 hr of collection.

Isotope Analysis

Samples of each species ($n = 5$) were dried at 60° C to constant weight. To remove carbonates, each sample was acidified with 1M HCl, rinsed with deionized water and dried at 60°C. Samples were ground with a mortar and pestle in liquid N₂. The carbon isotopic signature ($\delta^{13}\text{C}$) was determined for each sample using an isotope ratio mass spectrometer (Thermo Electron DeltaV Advantage) coupled with a CNS Elemental Analyzer (ConFlo II interface linked to a Carlo Erba NA 1500). All carbon isotopic results are expressed in standard delta notation relative to VPDB.

Statistical Analyses

All statistical tests were conducted using R (R Core Team 2013). Assumptions of normality of residuals and homogeneity of variance were tested using Shapiro Wilkes test and Levene's test respectively. For parameters where assumptions were not met, data was transformed with a log or square root transformation. In the case that assumptions were not met after transformations, a non-parametric test was used. For the pH and inhibitor experiments on *L. variegata* and *Peyssonnelia sp.* each response variable (α , P_{max} , P_{gmax} , I_c , and R) was tested in a separate ANOVA to see if there were significant differences

due to the pH and inhibitor treatment groups. A post hoc Tukey pairwise comparison test was used to determine which pH levels were significantly different from each other. A post hoc Dunnett's test was used on the inhibitor experiment to compare each inhibitor group to the control. For the second pH experiment on dominant reef macroalgae, one way ANOVA's were used for each response variable (NPP, GPP, and R). Isotope data was analyzed with a one-way ANOVA to determine if there were differences in $\delta^{13}\text{C}$ ratios between species. A post hoc Tukey pairwise comparison test was used to determine groupings of species with similar $\delta^{13}\text{C}$ ratios.

Results

L. variegata and Peyssonnelia sp. Experiments

pH Experiment

The pH treatments of high (8.5 pH), ambient (8.1 pH), levels projected by the year 2100 (7.8 pH), and low (7.5 pH), resulted in greater than an order of magnitude difference in CO_2 availability: 99, 349, 805 and 1740 ppm, respectively. Under these conditions, P_{max} and P_{gmax} were significantly affected by pH in *L. variegata* ($p < 0.05$, Tables 2.1, 2.2, Fig. 2.2). P_{max} was lowest at the high pH treatment of 8.5 and highest at the lowest pH level of 7.5. Compared to ambient pH (8.1), P_{max} increased by 36% when pH was reduced to 7.8, the level projected for 2100 (RCP 8.5, IPCC 2013) and more than doubled at the lowest pH tested (7.5). Photosynthetic rates were most affected by pH at saturating irradiance with no difference between treatments at sub-saturating irradiance (Fig. 2.2) supported by an insignificant p-value for α between pH treatments ($P > 0.05$, Table 2.2). In contrast, pH had no effect on P_{max} or P_{gmax} for *Peyssonnelia sp.* ($p > 0.05$, Tables 2.1, 2.2, Fig. 2.2). There were also no differences in α between pH treatments for

Peyssonnelia ($p > 0.05$, Table 2.2). The pH treatments had no effect on R or I_c ($p > 0.05$, Tables 2.1, 2.2, Fig. 2.2) for either species.

Inhibitor Experiment

Inhibiting the external CA with AZ reduced P_{max} significantly in both *L. variegata* and *Peyssonnelia sp.* ($P < 0.05$, Tables 2.3, 2.4, Fig 2.3). P_{max} was reduced by 56% in *L. variegata* and 60% in *Peyssonnelia sp.* (Table 2.3, Fig 2.3). *Peyssonnelia sp.* also showed sensitivity to two additional inhibitors that did not affect *L. variegata*. Inhibiting anion exchange proteins with PLP and inhibiting acidification of the boundary layer with Tris caused reductions of P_{max} in *Peyssonnelia sp.* ($P < 0.05$, Tables 2.3, 2.4, Fig 2.3), but not in *L. variegata* ($p > 0.05$, Tables 2.3, 2.4, Fig 2.3). Vanadate, an inhibitor of a P-Type ATPase proton pump, did not affect P_{max} for either *L. variegata* or *Peyssonnelia sp.* P_{gmax} , α , R, and I_c were unaffected by all inhibitors for both species ($P > 0.05$, Tables 2.3, 2.4, Fig 2.3).

Dominant Macroalgae pH Experiment

Change in pH and pCO_2 concentrations had differing effects on photosynthesis in the fleshy brown macroalgae studied. For *L. variegata* net photosynthesis was 56.6% higher at the pH projected for the year 2100 (7.8) compared to ambient pH (8.1) ($p < 0.05$); however, no reduction in photosynthesis occurred between high pH (8.5) and ambient (8.1) pH (Tables 2.5, 2.6). In the other brown macroalgae, *D. pulchella*, there were no statistically significant differences in net or gross photosynthetic rates across pH treatments ($P > 0.05$, Tables 2.5, 2.6).

Species of *Halimeda* also had differing photosynthetic responses to pH. *Halimeda gorreauii* and *H. opuntia* had higher net and gross photosynthesis in response to change

in pH and $p\text{CO}_2$ concentrations ($p < 0.05$, Tables 2.5, 2.6). In contrast, net and gross photosynthesis of *H. copiosa*, was unaffected by pH treatments ($P > 0.05$, Table 2.5, 2.6). Net and gross photosynthesis increased by 20% and 14% respectively in *H. tuna*, but was not statistically significant ($P > 0.05$, Tables 2.5, 2.6). This may be due to high variation between treatments. Respiration (R) was unaffected by pH for all species with the exception of *H. gorreauii*, which had higher respiration at lower pH ($p > 0.05$, Tables 2.5, 2.6).

Isotope Analysis

All species had $\delta^{13}\text{C}$ values less negative than -35 suggesting that they use HCO_3^- for photosynthesis, but may have different amounts of CO_2 that they acquire. Three statistically significant groupings of species emerged based on $\delta^{13}\text{C}$ signatures of photosynthetic (organic) tissue ($P < 0.05$, Figure 2.4). The first grouping was represented by the deepest reef species, *Peyssonnelia sp.*, which had the most negative $\delta^{13}\text{C}$ value of -25. A second grouping was the deep-water *Halimeda* species *H. opuntia*, *H. copiosa*, and *H. gorreauii* with an intermediate $\delta^{13}\text{C}$ signature of approximately -22. A third grouping was represented by the shallow reef species, including *H. tuna* and both fleshy brown species, *L. variegata* and *D. pulchella* which had a $\delta^{13}\text{C}$ value of approximately -17.

Discussion

Future conditions of $p\text{CO}_2$ and pH, consistent with projections for the year 2100, may increase photosynthesis in the brown, fleshy lobed dominant on Cayman Reefs, *L. variegata*, but not a dominant CCA, *Peyssonnelia*, based on short-term photophysiology experiments. One caveat is that short-term experiments do not always extrapolate to long term growth responses as species can acclimate to higher CO_2 concentrations (ref),

However, these data do offer one possible physiological driver for the increased abundance of fleshy macroalgal species as opposed to CCA in Caribbean reefs and in areas associated with naturally acidified CO₂ seeps (Enoch et al 2015). Higher abundance of fleshy macroalgae compared to calcified algae and corals has been observed along pH gradients near naturally acidified reefs (Fabricius et al 2011, Enochs et al 2015). In general, positive responses of fleshy macroalgae to OA contrast negative or neutral responses of calcified macroalgae seen in this and other studies (Johnson et al 2014; Comeau et al 2016), although these trends are not universal. In a few studies, crustose coralline algae have been found to show decreased growth rates or percent cover under experimental reductions of pH (Kuffner et al 2008; James et al 2014), but again, not uniformly (Dutra et al. 2015). Similarly, growth experiments indicate that some species of fleshy macroalgae have higher growth rates under elevated pCO₂ (Johnson et al 2014). Elevated pCO₂ has been found to increase the growth rate and competitive ability of *Lobophora papenfussii* over corals (Diaz-Pulido et al 2011). The increase in photosynthesis at a lower pH and greater CO₂ availability could be a physiological driver for increased competitive ability, growth, and proliferation of *Lobophora* sp. and other fleshy seaweeds in response to OA. Although brown fleshy macroalgae have been shown to dominate at field sites under low pH conditions (7.6 -7.8) within the range of my experiments (7.5-7.8), extremely low pH conditions (6.7 – 7.3 pH) can be detrimental to macroalgae, including *L. variegata* (Sangil et al 2016). Thus, the positive response of some fleshy species to elevated pCO₂ under OA may have limits.

When testing photosynthetic responses to elevated pCO₂ of other dominant macroalgae on Little Cayman Island reefs, different responses were found within genus,

functional form (fleshy vs. calcifiers) and irradiance environment. *Dictyota pulchella*, a prominent fleshy brown species dominant on Caribbean reefs (Liddel and Olhorst 1986, Edmunds 2002) did not increase photosynthesis at year 2100 pH levels (7.8) compared to ambient (8.1). This suggests that patterns cannot be broadly applied within functional groups of macroalgae. Even within the same genus, there were varying responses to elevated $p\text{CO}_2$ and lowered pH. Two species of *Halimeda* (*H. gorreauii* and *H. opuntia*) increased photosynthesis in response to elevated $p\text{CO}_2$ and lower pH, while photosynthetic rates remained unchanged or statistically insignificant in *H. tuna* and *H. copiosa*. Other studies of photosynthetic responses of *Halimeda* to elevated $p\text{CO}_2$ also found differing responses between species (Price et al 2011; Peach et al 2017). These results are consistent with the results of this study where *H. gorreauii* showed increased photosynthesis in response to elevated $p\text{CO}_2$, while *H. tuna* and *H. copiosa* had no significant differences in photosynthesis (Peach et al 2017). *Halimeda opuntia* was found to have increased photosynthesis in this study and Hoffman et al (2015) while approached significance ($p = 0.07$) in Peach et al (2017). However, *H. opuntia* was found to have lower or no difference in photosynthesis in studies which decreased pH to 7.7 - 7.8 and were run at lower light levels (Price et al 2011, Johnson et al 2014, Vogel et al 2015). These species-specific responses to OA can be better understood in the context of carbon use strategies, as identified by inhibitor experiments for *L. variegata* and *Peyssonnelia sp.*, and isotopic signatures of the dominant reef macroalgae examined.

Based on inhibitor experiments and carbon isotopic signatures ($\delta^{13}\text{C}$), all algae tested were able to use HCO_3^- . All algae had $\delta^{13}\text{C}$ above -30‰, which indicated HCO_3^- use was part of each species' inorganic carbon uptake strategy (Maberly et al 1992;

Raven et al 2002). The use of HCO_3^- found in dominant tropical species in this study supports previous literature that revealed the use of HCO_3^- as a source of inorganic carbon was widespread among different phyla and functional groups of macroalgae (Maberly et al 1992; Koch et al 2013).

Inhibitor experiments for *L. variegata* and *Peyssonnelia sp.* offered more specific evidence of their carbon uptake mechanisms including the first evidence for anion-exchange proteins used in the active uptake of HCO_3^- in tropical red macroalgae. External CA used to dehydrate external HCO_3^- to CO_2 was identified as a key strategy for both *Peyssonnelia sp.* and *L. variegata*. This offers further evidence that external CA is a widespread carbon uptake mechanism amongst diverse groups (CCA and lobed fleshy brown algae). Furthermore, contrary to my a priori hypothesis that *Peyssonnelia* may lack active carbon uptake strategies, it presented a greater number of active carbon uptake mechanisms than *L. variegata*. Its sensitivity to PLP indicated the presence of an AE protein and an active uptake mechanism. So far, the use of AE proteins for active uptake of HCO_3^- had only been shown in a few macroalgae, including fleshy temperate species, *Enteromorpha intestinalis*, *Macrocystis pyrifera*, and some in the genus *Ulva* (Drechsler et al 1993; Fernandez et al 2014; Rautenberger et al 2015). An active uptake mechanism in *Peyssonnelia* is surprising because of its presence in low-light environments and active uptake mechanisms are energetically expensive (Hepburn et al. 2011, Raven et al 2014). *Peyssonnelia* was also sensitive to Tris buffer, which blocks the acidification of the boundary layer. These data indicate that *Peyssonnelia* is able to influence its pH microenvironment at the surface boundary layer in ways that facilitate photosynthesis. However, *Peyssonnelia* was not sensitive to Vanadate, which tests for a P-type ATP-ase

proton pump. A P-type ATP-ase proton pump has been suggested as a way some algae are able to lower pH by active pumping of H^+ (Giordano et al 2005; Mercado et al 2006). The lack of sensitivity to Vanadate suggests *Peyssonnelia* may be using other mechanisms to control boundary layer pH. A second interesting finding was that, although *Peyssonnelia* had more inorganic carbon uptake mechanisms identified by inhibitor experiments, it had the lowest HCO_3^- use in the field indicated by its $\delta^{13}C$ signature. This suggests that it may have the ability to use CCM's, but may not utilize them to the same degree in low-irradiance environments compared to algae in high-irradiance environments. This supposition, that algae capable of CCM's may not depend on them in low-irradiance environments, was supported in mesocosm experiments with *Ulva* grown in high- and low-irradiance treatments. *Ulva* grown in high irradiance treatments had higher isotopic signatures than algae grown in low-irradiance treatments, suggesting that CCM use may be facultative and preferentially used under high-irradiance (Rautenberger et al 2015). The finding that algae may be using more CCM's at high light is also supported by findings based on PI curves in my inhibitor experiments. Differences in photosynthetic rates attributed to inhibitors were more prominent at saturating than sub-saturating irradiance. This is also supported by the non-significant effect of inhibitors on α for both species.

Related to light availability, depth at which individual species dominate and grow influenced the carbon use strategies they employ. Based on $\delta^{13}C$ ratios, algae found in deep, low-light environments used more CO_2 than HCO_3^- . Algae growing under shelves and in low-light conditions on the reef, such as *Peyssonnelia*, *H. copiosa*, *H. gorreuii*, and *H. opuntia*, had lower $\delta^{13}C$ ratios than algae, such as *H. tuna*, *L. variegata*, and *D.*

pulchella, found in shallow reefs on Little Cayman Island. Thus, deeper species appear to rely more heavily on CO₂. The same pattern of δ¹³C ratios being lower at greater depths has been found in other reef systems such as the Great Barrier Reef where algae were collected along a depth gradient, albeit shallower (1 – 10 m; Diaz-Pulido et al 2016) than in the present study (12 – 19 m). These data are consistent with the interpretation that CO₂ and HCO₃⁻ use for photosynthesis is linked to CO₂ availability and/or irradiance. This is possibly due to the energetic costs associated with using CCMs. At lower light levels, species may be meeting their inorganic carbon needs for maximum photosynthesis with less HCO₃⁻ use than those in higher light environments. No significant difference was found for α, where light is under saturated with respect to photosynthesis, for both *L. variegata* and *Peyssonnelia*. Blocking CA and active uptake of HCO₃⁻ under low irradiance did not limit photosynthesis, regardless of the uptake mechanism. Additionally, deeper waters can be enriched by upwelling of CO₂ rich water (Strong et al 2014). In contrast to low-light conditions, species under high irradiance are able to utilize a greater proportion of HCO₃⁻.

Contrary to the a priori hypothesis that species using HCO₃⁻ would be less affected by OA, there were no patterns between the use of HCO₃⁻ and effects of elevated *p*CO₂ and lower pH on photosynthesis. In contrast, all species studied indicated some use of HCO₃⁻ based on δ¹³C values, and 42% of species studied increased photosynthesis at elevated *p*CO₂. These results indicate that even species with the ability to use HCO₃⁻ may be carbon limited at ambient seawater DIC levels (~2000 μmol kg⁻¹) exhibiting increased photosynthesis in response to OA. This is contrary to some hypotheses in the literature, which suggest that species using HCO₃⁻ via CCM's do not increase photosynthetic rates

in response to elevated $p\text{CO}_2$ (Israel and Hophy 2002). One reason why species that use HCO_3^- may respond positively to increased CO_2 and lower pH is that under low pH conditions CA shifts to favoring dehydration of HCO_3^- . This equilibrium shift towards more CO_2 with greater OA could promote species using CA to provide inorganic carbon for photosynthesis. Additionally, species in shallow reefs may be carbon limited during parts of the diurnal cycle when pH rises due to increased photosynthesis on reefs during the day (Andersson and Mackenzie 2012). In Little Cayman Island reefs, pH was found to fluctuate from 8.08 at 08:00 hr. to 8.29 at 18:00 hr. (375-675 ppm CO_2 , Peach et al 2017). The $\delta^{13}\text{C}$ data provided further evidence that species' photosynthetic responses to elevated CO_2 may not be linked to their ability to use HCO_3^- . *Peyssonnelia* had the lowest $\delta^{13}\text{C}$ signature, indicating it used more CO_2 proportionally than other species. Previous literature suggests that species that have a high dependence on CO_2 and low utilization of HCO_3^- such as *Peyssonnelia* would have more of an ability to respond to OA (Kübler 1999), however, this was not the case in this study. *Peyssonnelia*'s lack of response to increased $p\text{CO}_2$ may be due to it requiring less inorganic carbon for maximum photosynthetic rates. In an earlier study, *Peyssonnelia* sp. from Little Cayman was found to have a 62% lower P_{max} than *L. variegata* based on P:I curves normalized to surface area (Koch unpublished data).

In conclusion, irradiance and CO_2 availability as a function of depth are proposed as two of the most significant factors controlling the photosynthetic response of tropical macroalgae to OA. This supposition is supported by the fact that no significant differences were found at sub-saturating light (α) across a range of pH and CO_2 availability, even when multiple inhibitors constrained various bicarbonate uptake

mechanisms. In contrast, significant differences in photosynthetic maxima were found at light saturation in several species examined. Stable isotope signatures provide additional evidence that bicarbonate use is dominant in species residing in shallow, high-irradiance locations on Little Cayman Reefs. Although a dominance of bicarbonate use was most pronounced at shallow depths, all species used bicarbonate and no obligate CO₂ users were identified by $\delta^{13}\text{C}$ and inhibitor experiments. Interestingly, the CCA species examined, *Peyssonnelia* sp., did not respond to elevated $p\text{CO}_2$ even at light saturation, compared to *L. variegata* which had a significantly greater photosynthetic rate at 7.5 compared to 8.1 and 8.5 pH. Along with its relatively high photosynthetic rate, and wide distribution across irradiance gradients in comparison to *Peyssonnelia* sp. (Koch unpublished data), *L. variegata* has been shown here to have an enhanced photosynthetic rate in response to higher $p\text{CO}_2$ at light saturation. Thus, future conditions of OA may perpetuate or exacerbate the abundance of fleshy seaweeds such as *L. variegata* on Caribbean reefs. This potential expansion of fleshy species, however, will be species-specific. Another dominant brown macroalgae on tropical reefs, *D. pulchella* did not increase productivity under low pH treatments, relative to controls. Finally, the *Halimeda* genus with several important species in tropical reef ecosystems exhibits species-specific responses to OA as shown in this study, those by Price (2011) and Peach et al. (2017), indicating positive photosynthetic responses, principally P_{max} , to OA by *H. gorreauii* and *opuntia* and no response by *H. copiosa* and *tuna*. Saturating light conditions were important in regulating any potential enhancement of tropical macroalgal photosynthesis to OA; however, the dominant response pattern was species-specific, indicating that

much work will be required to identify which dominant tropical reef macroalgae will be able to increase photosynthesis with rising $p\text{CO}_2$ in the oceans.

Appendices

Appendix 1 – Tables

Table 1.1. Calculated (CO2sys, Pierrot et al 2006) inorganic carbon speciation ($\mu\text{mol kg}^{-1}$) for pH treatments using average salinity from in situ seawater and temperature, alkalinity, and pH adjustments from incubation seawater. CO2 concentrations for each treatment in ppm are 127ppm (8.5), 334ppm (8.1), 741ppm (7.8), and 1645ppm (7.5).

pH	CO ₂	HCO ₃ ⁻	CO ₃ ²⁻
7.5	43.35	2160.55	85.3
7.8	19.40	1983.6	161.1
8.1	8.95	1773.95	276.55
8.5	3.35	1531.14	540.40

Table 1.2. Average (\pm SE) gross maximum photosynthesis (P_{gmax} $\mu\text{mol O}_2 \text{ g}^{-1} \text{ min}^{-1}$), net maximum photosynthesis (P_{max} $\mu\text{mol O}_2 \text{ g}^{-1} \text{ min}^{-1}$), respiration (R $\mu\text{mol O}_2 \text{ g}^{-1} \text{ min}^{-1}$) photosynthetic efficiency (α $\mu\text{mol O}_2 / \mu\text{mol photons}$), and light compensation point (I_c $\mu\text{mol photons m}^{-2} \text{ s}^{-1}$) at pH 7.5, 7.8, 8.1, and 8.5. Photosynthetic parameters were calculated using the hyperbolic tangent equation (Jassby and Platt 1976). Different letters denote significant differences among pH treatments ($P < 0.05$).

	P_{gmax}	P_{max}	R	α	I_c
<i>Canistrocarpus cervicornis</i>					
7.5	0.55 \pm 0.03 ^a	0.32 \pm 0.04 ^a	0.23 \pm 0.03	2.0E-3 \pm 2.7E-4	144 \pm 40
7.8	0.42 \pm 0.03 ^b	0.20 \pm 0.03 ^b	0.22 \pm 0.01	2.4E-3 \pm 3.7E-4	118 \pm 25
8.1	0.31 \pm 0.03 ^{bc}	0.09 \pm 0.02 ^{bc}	0.22 \pm 0.01	2.0E-3 \pm 5.7E-4	190 \pm 56
8.5	0.25 \pm 0.03 ^c	-0.02 \pm 0.02 ^c	0.27 \pm 0.03	2.6E-3 \pm 8.6E-4	167 \pm 61
<i>CCA</i>					
7.5	0.011 \pm 0.001	0.008 \pm 0.002	0.003 \pm 0.000	5.0E-5 \pm 4.5E-6	71 \pm 11
7.8	0.014 \pm 0.002	0.010 \pm 0.002	0.004 \pm 0.001	4.8E-5 \pm 7.7E-6	128 \pm 37
8.1	0.013 \pm 0.002	0.009 \pm 0.002	0.004 \pm 0.001	6.2E-5 \pm 1.1E-5	107 \pm 47
8.5	0.012 \pm 0.001	0.008 \pm 0.001	0.003 \pm 0.001	5.9E-5 \pm 1.3E-5	68 \pm 10
<i>Halimeda opuntia</i>					
7.5	0.21 \pm 0.019 ^a	0.17 \pm 0.017 ^a	0.05 \pm 0.004	5.1E-4 \pm 6.4E-5	104 \pm 12 ^a
7.8	0.14 \pm 0.011 ^b	0.08 \pm 0.009 ^b	0.06 \pm 0.006	5.1E-4 \pm 7.8E-5	144 \pm 22 ^{ab}
8.1	0.11 \pm 0.013 ^b	0.06 \pm 0.013 ^b	0.05 \pm 0.004	3.1E-4 \pm 7.1E-5	216 \pm 28 ^b
8.5	0.07 \pm 0.004 ^c	0.01 \pm 0.004 ^c	0.06 \pm 0.004	3.1E-4 \pm 7.2E-5	454 \pm 67 ^c
<i>Jania adhaerens</i>					
7.5	0.70 \pm 0.04 ^a	0.61 \pm 0.03 ^a	0.09 \pm 0.01	1.1E-3 \pm 9.9E-5	85 \pm 9
7.8	0.64 \pm 0.06 ^{ab}	0.54 \pm 0.06 ^{ab}	0.10 \pm 0.02	9.8E-4 \pm 1.1E-4	119 \pm 28
8.1	0.56 \pm 0.03 ^{ab}	0.48 \pm 0.03 ^{ab}	0.08 \pm 0.01	9.5E-4 \pm 7.7E-5	83 \pm 7
8.5	0.50 \pm 0.03 ^b	0.41 \pm 0.02 ^b	0.09 \pm 0.01	1.0E-3 \pm 4.2E-5	90 \pm 14
<i>Laurencia intricata</i>					
7.5	0.77 \pm 0.05 ^a	0.62 \pm 0.05 ^a	0.15 \pm 0.01	1.6E-3 \pm 1.6E-4 ^a	99 \pm 13 ^{ab}
7.8	0.63 \pm 0.04 ^{ab}	0.53 \pm 0.04 ^{ab}	0.10 \pm 0.01	1.3E-3 \pm 1.2E-4 ^{ab}	84 \pm 11 ^a
8.1	0.57 \pm 0.06 ^b	0.48 \pm 0.05 ^{ab}	0.09 \pm 0.01	1.1E-3 \pm 1.2E-4 ^{ab}	83 \pm 11 ^a
8.5	0.49 \pm 0.06 ^b	0.37 \pm 0.06 ^b	0.12 \pm 0.01	0.8E-3 \pm 1.0E-4 ^b	151 \pm 19 ^b
<i>Neogoniolithon strictum</i>					
7.5	0.21 \pm 0.02	0.18 \pm 0.01	0.04 \pm 0.004	3.8E-4 \pm 3.3E-5	97 \pm 11
7.8	0.21 \pm 0.02	0.17 \pm 0.02	0.04 \pm 0.005	4.2E-4 \pm 4.9E-5	112 \pm 16
8.1	0.17 \pm 0.02	0.14 \pm 0.01	0.03 \pm 0.004	4.0E-4 \pm 2.7E-5	87 \pm 11
8.5	0.20 \pm 0.03	0.15 \pm 0.02	0.05 \pm 0.009	4.0E-4 \pm 6.4E-5	130 \pm 16
<i>Sargassum fluitans</i>					
7.5	0.54 \pm 0.04 ^a	0.30 \pm 0.03	0.24 \pm 0.01 ^{ab}	3.2E-3 \pm 2.1E-4 ^a	81 \pm 3
7.8	0.49 \pm 0.04 ^{ab}	0.22 \pm 0.04	0.27 \pm 0.03 ^a	3.1E-3 \pm 7.8E-4 ^a	114 \pm 21
8.1	0.43 \pm 0.01 ^{ab}	0.22 \pm 0.01	0.21 \pm 0.02 ^{ab}	1.4E-3 \pm 3.2E-4 ^{ab}	232 \pm 101
8.5	0.33 \pm 0.06 ^b	0.16 \pm 0.04	0.17 \pm 0.03 ^b	1.0E-3 \pm 5.8E-4 ^b	297 \pm 78

Udotea luna

7.5	1.08 ± 0.11^a	0.57 ± 0.11^a	0.50 ± 0.04	$4.3E-3 \pm 9.3E-4^a$	149 ± 18^a
7.8	0.99 ± 0.13^{ab}	0.48 ± 0.07^{ab}	0.51 ± 0.09	$4.5E-3 \pm 1.3E-3^{ab}$	148 ± 23^a
8.1	0.68 ± 0.05^b	0.26 ± 0.05^b	0.42 ± 0.02	$2.3E-3 \pm 1.0E-4^b$	236 ± 24^b
8.5	0.75 ± 0.04^{ab}	0.20 ± 0.05^b	0.55 ± 0.03	$3.7E-3 \pm 3.6E-4^{ab}$	203 ± 15^{ab}

Table 1.3. One-Way ANOVA results on net photosynthesis maxima (P_{\max}), gross photosynthesis maxima ($P_{g\max}$), photosynthetic efficiency (α), respiration (R) and light compensation point (I_c) in response to pH treatments. Significant effects ($p < 0.05$) are marked with an asterisk.

	Df	Sum Sq	Mean Sq	F-value	p-value
<i>Canistrocarpus cervicornis</i>					
$P_{g\max}$	3	0.25791	0.08597	20.65	9.52e-06*
P_{\max}	3	0.31076	0.10359	25.37	2.54e-06*
R	3	0.00815	0.002716	1.073	0.388
α	3	1.617e-06	5.391e-07	0.338	0.798
I_c	3	13575	4525	0.51	0.682
CCA					
$P_{g\max}$	3	0.0000391	1.302e-05	0.676	0.574
P_{\max}	3	0.0000116	3.856e-06	0.208	0.89
R	3	0.000455	0.0001517	0.748	0.533
α	3	1.228e-09	4.093e-10	0.535	0.662
I_c	3	0.1504	0.05014	0.519	0.673
<i>Halimeda opuntia</i>					
$P_{g\max}$	3	0.16070	0.05357	23.18	9.59e-08*
P_{\max}	3	0.3347	0.11157	35.73	1.04e-09*
R	3	0.001075	0.0003583	2.073	0.126
α	3	3.181e-07	1.061e-07	2.586	0.073
I_c	3	1.6296	0.5432	16.5	2.73e-06*
<i>Jania adhaerens</i>					
$P_{g\max}$	3	0.1824	0.06079	4.531	0.0104*
P_{\max}	3	0.08057	0.026858	4.156	0.0148*
R	3	0.00266	0.0008882	0.681	0.571
α	3	5.660e-08	1.886e-08	0.317	0.813
I_c	3	6717	2239	1.035	0.392
<i>Laurencia intricata</i>					
$P_{g\max}$	3			9.6251	0.02204 ⁱ *
P_{\max}	3	0.2058	0.06861	5.465	0.00551*
R	3	0.01580	0.005267	1.499	0.241
α	3	1.869e-06	6.229e-07	3.279	0.0392*
I_c	3	19102	6367	4.612	0.0114*
<i>Neogoniolithon strictum</i>					
$P_{g\max}$	3	0.00932	0.003108	0.946	0.432
P_{\max}	3	0.00818	0.002727	1.161	0.342
R	3	0.001029	0.0003430	1.292	0.297
α	3	4.200e-09	1.411e-09	0.085	0.968
I_c	3	8378	2793	1.831	0.164
<i>Sargassum fluitans</i>					
$P_{g\max}$	3	0.09566	0.03189	4.908	0.0188*

P_{\max}	3	0.04143	0.013810	3.241	0.0603
R	3	0.02420	0.008067	4.601	0.023*
α	3	1.502e-05	5.006e-06	4.602	0.023*
I_c	3	122441	40814	2.44	0.115
<i>Udotea luna</i>					
$P_{g\max}$	3	0.6387	0.21289	4.226	0.0182*
P_{\max}	3	0.5566	0.18553	5.69	0.00551*
R	3			4.9333	0.1767 ⁱ
α	3	0.04497	0.014990	4.288	0.0172*
I_c	3	33900	11300	4.487	0.0145*

ⁱKruskal-Wallis rank sum test

Table 1.4. Average (\pm SE) gross maximum photosynthesis (P_{\max} $\mu\text{mol O}_2 \text{g}^{-1} \text{min}^{-1}$), net maximum photosynthesis ($P_{g\max}$ $\mu\text{mol O}_2 \text{g}^{-1} \text{min}^{-1}$), respiration (R $\mu\text{mol O}_2 \text{g}^{-1} \text{min}^{-1}$) photosynthetic efficiency (α $\mu\text{mol O}_2 \mu\text{mol}^{-1}$ photons), and light compensation point (I_c $\mu\text{mol photons m}^{-2} \text{s}^{-1}$) in the presence of four inhibitors (AZ, PLP, Tris, and Van) and control. Inhibitors with a significant effect ($p < 0.05$) relative to control are marked with asterisks. Parameters were calculated using the hyperbolic tangent equation (Jassby and Platt 1976).

	$P_{g\max}$	P_{\max}	R	α	I_c
<i>Canistrocarpus Cervicornis</i>					
Control	0.39 \pm 0.04	0.17 \pm 0.02	0.22 \pm 0.04	2.3E-3 \pm 4.2E-4	118 \pm 15
AZ	0.25 \pm 0.02*	0.08 \pm 0.02*	0.17 \pm 0.02	2.0E-3 \pm 5.3E-4	162 \pm 56
PLP	0.43 \pm 0.05	0.19 \pm 0.04	0.24 \pm 0.03	1.9E-3 \pm 5.7E-4	230 \pm 50
Tris	0.44 \pm 0.03	0.23 \pm 0.04	0.20 \pm 0.03	2.1E-3 \pm 3.3E-4	139 \pm 31
Van	0.31 \pm 0.02	0.17 \pm 0.02	0.14 \pm 0.01	1.9E-3 \pm 2.2E-4	91 \pm 11
CCA					
Control	0.014 \pm 0.001	0.012 \pm 0.001	0.002 \pm 0.000	6.1E-5 \pm 8.2E-6	34 \pm 5
AZ	0.007 \pm 0.001	0.005 \pm 0.001	0.002 \pm 0.001	5.2E-5 \pm 2.3E-5	143 \pm 64
PLP	0.013 \pm 0.002	0.006 \pm 0.002	0.006 \pm 0.001	6.6E-5 \pm 1.2E-5	61 \pm 20
Tris	0.012 \pm 0.002	0.003 \pm 0.001	0.003 \pm 0.001	5.2E-5 \pm 4.4E-6	48 \pm 13
Van	0.013 \pm 0.003	0.002 \pm 0.002	0.002 \pm 0.001	8.0E-5 \pm 2.3E-5	29 \pm 6
<i>Halimeda opuntia</i>					
Control	0.12 \pm 0.01	0.06 \pm 0.01	0.06 \pm 0.01	7.1E-4 \pm 2.8E-4	174 \pm 34
AZ	0.10 \pm 0.01	0.02 \pm 0.01*	0.07 \pm 0.01	2.8E-4 \pm 5.1E-5	372 \pm 42*
PLP	0.12 \pm 0.01	0.05 \pm 0.01	0.07 \pm 0.01	5.1E-4 \pm 4.3E-5	186 \pm 22
Tris	0.12 \pm 0.01	0.05 \pm 0.01	0.07 \pm 0.00	3.8E-4 \pm 1.5E-4	284 \pm 49
Van	0.09 \pm 0.01	0.03 \pm 0.00	0.06 \pm 0.01	4.0E-4 \pm 8.8E-5	196 \pm 31
<i>Jania adhaerens</i>					
Control	0.55 \pm 0.04	0.48 \pm 0.04	0.07 \pm 0.01	1.3E-3 \pm 1.8E-4	60 \pm 10
AZ	0.19 \pm 0.02*	0.08 \pm 0.01*	0.10 \pm 0.02	1.7E-3 \pm 4.4E-4	91 \pm 23
PLP	0.36 \pm 0.04*	0.30 \pm 0.04*	0.05 \pm 0.01	1.2E-3 \pm 1.3E-4	48 \pm 10
Tris	0.49 \pm 0.03	0.44 \pm 0.03	0.05 \pm 0.01	1.1E-3 \pm 7.2E-5	45 \pm 7
Van	0.51 \pm 0.05	0.44 \pm 0.05	0.07 \pm 0.00	1.3E-3 \pm 1.6E-4	55 \pm 8
<i>Laurencia intricata</i>					
Control	0.50 \pm 0.03	0.40 \pm 0.03	0.11 \pm 0.01	8.6E-4 \pm 6.4E-5	130 \pm 12
AZ	0.34 \pm 0.02*	0.20 \pm 0.02*	0.14 \pm 0.01	8.8E-4 \pm 9.4E-5	185 \pm 19
PLP	0.33 \pm 0.06*	0.16 \pm 0.06*	0.17 \pm 0.02*	8.1E-4 \pm 1.9E-4	240 \pm 53
Tris	0.29 \pm 0.02*	0.13 \pm 0.02*	0.16 \pm 0.02*	1.4E-3 \pm 4.0E-4	214 \pm 65
Van	0.29 \pm 0.05*	0.18 \pm 0.05*	0.11 \pm 0.01	1.0E-3 \pm 7.9E-5	127 \pm 14
<i>Neogoniolithon strictum</i>					

Control	0.18 ± 0.01	0.12 ± 0.01	0.07 ± 0.01	2.8E-4 ± 3.5E-5	297 ± 50
AZ	0.19 ± 0.03	0.11 ± 0.02	0.08 ± 0.02	3.4E-4 ± 5.8E-5	275 ± 62
PLP	0.17 ± 0.02	0.10 ± 0.02	0.07 ± 0.01	2.8E-4 ± 3.7E-5	326 ± 68
Tris	0.17 ± 0.01	0.10 ± 0.01	0.07 ± 0.01	3.1E-4 ± 2.8E-5	237 ± 27
Van	0.17 ± 0.02	0.11 ± 0.02	0.06 ± 0.01	2.7E-4 ± 2.8E-5	218 ± 12
<hr/>					
<i>Sargassum fluitans</i>					
Control	0.57 ± 0.06	0.41 ± 0.07	0.16 ± 0.01	2.7E-3 ± 4.1E-4	72 ± 15
AZ	0.19 ± 0.04*	0.02 ± 0.04*	0.17 ± 0.01	2.1E-3 ± 5.2E-4	-
PLP	0.39 ± 0.06	0.23 ± 0.06	0.16 ± 0.03	2.6E-3 ± 7.2E-4	79 ± 11
Tris	0.40 ± 0.05	0.21 ± 0.05	0.19 ± 0.02	2.9E-3 ± 3.3E-4	83 ± 16
Van	0.55 ± 0.07	0.33 ± 0.06	0.21 ± 0.03	3.2E-3 ± 5.4E-4	100 ± 34
<hr/>					
<i>Udotea luna</i>					
Control	0.61 ± 0.10	0.28 ± 0.06	0.33 ± 0.05	2.9E-3 ± 4.8E-4	135 ± 7
AZ	0.36 ± 0.04*	-0.03 ± 0.02*	0.39 ± 0.06	3.6E-3 ± 1.0E-3	223 ± 24
PLP	0.52 ± 0.05	0.16 ± 0.05	0.37 ± 0.04	3.0E-3 ± 6.1E-4	155 ± 20
Tris	0.42 ± 0.04	0.01 ± 0.02*	0.40 ± 0.06	2.9E-3 ± 5.7E-4	263 ± 21
Van	0.64 ± 0.06	0.31 ± 0.04	0.34 ± 0.03	2.5E-3 ± 5.5E-4	203 ± 29

Table 1.5. One-Way ANOVA table for inhibitors effects on net photosynthesis maxima (P_{\max}), gross photosynthesis maxima ($P_{g\max}$), photosynthetic efficiency (α), respiration (R) and light compensation point (I_c). In cases where the assumption of homogeneity of variances was not met a non-parametric Kruskal-Wallis test was used (i). Significant effects ($p < 0.05$) are marked with an asterisk.

	Df	Sum Sq	Mean Sq	F-value	p-value
<i>Canistrocarpus cervicornis</i>					
$P_{g\max}$	4	0.02141	0.005352	6.32	6.49 E-4*
P_{\max}	4	0.1763	0.04408	4.406	0.00562*
R	4	0.05185	0.012963	1.978	0.12
α	4	0.000182	4.549e-05	0.269	0.896
I_c	4	0.4475	0.11188	1.328	0.28
CCA					
$P_{g\max}$	4	0.005196	0.0012991	2.626	0.051
P_{\max}	4	0.0002523	6.309e-05	3.46	0.0175*
R	4	0.004073	0.0010182	2.018	0.113
α	4	1.853e-05	4.632e-06	0.788	0.541
I_c	4	1.041	0.2601	1.913	0.13
<i>Halimeda opuntia</i>					
$P_{g\max}$	4	0.005921	0.0014804	1.599	0.198
P_{\max}	4	0.00575	0.001437	2.995	0.0326*
R	4	8.170e-07	2.043e-07	1.102	0.372
α	4	0.0003989	9.972e-05	1.62	0.192
I_c	4	188376	47094	4.926	0.00343 *
<i>Jania adhaerens</i>					
$P_{g\max}$	4	0.6918	0.17295	16.95	8.1e-08*
P_{\max}	4	0.8357	0.20893	19.08	2.1e-08*
R	4	0.01516	0.003790	3.635	0.014*
α	4	-	-	2.2244	0.6946 ⁱ
I_c	4	11086	2772	2.053	0.108
<i>Laurencia intricata</i>					
$P_{g\max}$	4	0.2560	0.06400	4.652	0.0042 *
P_{\max}	4	0.3773	0.09433	7.733	0.00015 *
R	4	0.04518	0.011295	3.629	0.014*
α	4	2.107e-06	5.268e-07	1.561	0.207
I_c	4	0.2866	0.07165	1.894	0.136
<i>Neogoniolithon strictum</i>					
$P_{g\max}$	4	0.00355	0.0008873	0.35	0.842
P_{\max}	4	0.00163	0.0004065	0.241	0.913
R	4	-	-	3.0585	0.5481 ⁱ
α	4	2.24e-08	5.592e-09	0.467	0.759
I_c	4	61062	15265	0.806	0.53
<i>Sargassum fluitans</i>					
$P_{g\max}$	4	0.5426	0.13565	11.72	4.95e-06*

P_{\max}	4			23.2344	0.0001137 [†]
R	4	0.03798	0.009494	3.023	0.031
α	4	1.438e-05	3.596e-06	1.824	0.148
I_c	3	4110	1370	1.118	0.36
<i>Udotea luna</i>					
$P_{g\max}$	4	0.03634	0.009085	3.498	0.0167*
P_{\max}	4	0.7409	0.1852	12.6	1.9e-06*
R	4	0.0349	0.008735e-5	0.483	0.748
α	4	4.780e-06	1.195e-06	0.321	0.862
I_c		No hov			

Table 1.6. Two -Way ANOVA table for the combined effects of pH and AZ on gross photosynthesis maxima (P_{gmax}) for *C. cervicornis* and *J. adhaerens*. Significant effects ($p < 0.05$) are marked with an asterisk.

	df	Sum sq	Mean sq	F-value	p-value
<i>Canistrocarpus cervicornis</i>					
AZ	1	0.3363	0.3363	31.282	6.91e-07*
pH	3	1.4517	0.4839	45.004	6.15e-15*
AZ x pH	3	0.0327	0.0109	1.013	0.394
<i>Jania adhaerens</i>					
AZ	1	0.19462	0.19462	23.631	3.2e-05*
pH	3	0.10139	0.03380	4.104	0.0146*
AZ x pH	3	0.03562	0.01187	1.442	0.2496

Table 1.7. Synthesis of research on photosynthesis in marine macroalgae in response to ocean acidification. Species are grouped by phyla and labeled calcified (c) or fleshy (f). The effect of increased $p\text{CO}_2$ on photosynthesis is labeled as positive (+), negative (-), parabolic (p) or neutral (o). Studies were reported that included pH and $p\text{CO}_2$ ranges consistent with ambient and projected levels by 2100

Phylum (<i>Species</i>)	c/f	pH range	CO_2 range	OA effect	Citation(s)
Chlorophyta					
<i>Halimeda discoidea</i>	c	491 – 1201		+	1
<i>H. copiosa</i>	c	7.89 – 8.29	375-1087	o	25
<i>H. cylindracea</i>	c			-	2
<i>H. gorraeuii</i>	c	7.89 – 8.29	375-1087	+	25
<i>H. incrassata</i>	c	7.89 – 8.29	375-1087	o	25
<i>H. macroloba</i>	c		494 – 2000	o/-	2,3
<i>H. minima</i>	c		494 – 2000	o	3
<i>H. monile</i>	c	7.89 – 8.29	375-1087	o	25
<i>H. opuntia</i>	c	7.89 – 8.29	375-1087	o/-	4,5,6,7,25
	c	7.5-8.5	127-1645	+	This study
<i>H. taenicola</i>	c			o	4,5
<i>H. tuna</i>	c	7.89 – 8.29	375-1087	o	25
<i>Udotea luna</i>	c	7.5-8.5	127-1645	+	This study
<i>Ulva lactuca</i>	f			+	8
<i>U. prolifera</i>	f			+	9
<i>U. pulchra</i>	f			-	10
<i>U. reticulata</i>	f			-	10
<i>U. sp.</i>	f	7.5 – 7.9		o	12
Ochrophyta					
<i>Alaria esculenta</i>	f	7 – 10		+	13
<i>Ascophyllum nodosum</i>	f	7 – 10	400 – 800	+	13,14
<i>Canistrocarpus cervicornis</i>	f	7.5-8.5	127-1645	+	This study
<i>Endarachne binghamiae</i>	f			o	15
<i>Feldmannia spp.</i>	f			+	16
<i>Fucus seratus</i>	f	7 – 10		+	13
<i>F. spiralis</i>	f	7 – 10	400 – 800	o/+	13,14
<i>F. vesiculosus</i>	f	7 – 10		+	13
<i>Halydrys siliquosa</i>	f	7 – 10		+	13
<i>Hizikia fusiformis</i>	f			+	17
<i>Laminaria digitada</i>	f	7 – 10		+	13
<i>L. hyperborea</i>	f	7 – 10		+	13
<i>L. sacharina</i>	f	7 – 10		+	13

<i>Lobophora variegata</i>	f	7 – 9		+	18
<i>Macrocystis pyrifera</i>	f			+	19
<i>Padina sanctae</i> <i>cruces</i>	c	7 – 9		o	18
<i>Palmaria palmate</i>	f			-	21
<i>Pelvetia canaliculata</i>	f	7 – 9	400 – 800	+	13,14
<i>Sacharina latissima</i>	f		400 – 800	+	14, 21
<i>Sargassum fluitans</i>	f	7.5-8.5	127-1645	+	This study
<i>S. muticum</i>	f		400 – 800	+	14
<i>Undaria pinnatifida</i>	f	7.5 – 7.9		o	12

Rhodophyta

<i>Arthrocardia</i> <i>corymbosa</i>	c			o	24
<i>Corallina officinalis</i>	c	7.5 – 7.9		o/-	12,6,29
<i>C. sessilis</i>	c	7.9-8.4	380-1000	-	27
<i>Hydrolithon onkodes</i>	c		494 – 2000	o	5
<i>Hydrolithon</i> <i>reinboldii</i>	c		494 – 2000	o	3
<i>Hydrolithon sp</i>	c	7.5-10		+/0	28
<i>Jania adhaerens</i>	c	7.5-8.5	127-1645	+	This study
<i>Lithophyllum</i> <i>kotschyannum</i>	c		494 – 2000	o	3
<i>Lithothamnion</i> <i>corallinoides</i>	c	7.68-8.09	380-1000uatm	+	25
<i>L. flavescens</i>	c		494 – 2000	o	3
<i>Laurencia intricata</i>	f	7.5-8.5	127-1645	+	This study
<i>Neogoniolithon</i> <i>frutescens</i>	c		494 – 2000	o	3
<i>N. strictum</i>	c	7.5-8.5	127-1645	o	This study
<i>Neosiphonia harveyi</i>	f		406 - 1411	+	8
<i>Porolithon onkodes</i>	c		494 - 2000	o/	3,22
<i>Porphyra leucostica</i>	f			p	23
<i>Porphyra yezoensis</i>	f		380-1600	+	26
<i>Rhodophyllis gunnii</i>	f	7.5 - 7.9		o	12
<i>Schizoseris sp.</i>	f	7.5 - 7.9		o	12

Citations are as follows: (1) Peach et al 2016, (2) Sinotok et al 2011, (3) Comeau et al 2016, (4) Price et al 2011, (5) Johnson et al 2014, (6) Hofmann et al 2014, (7) Vogel et al 2015 (8) Olischläger et al 2013 (9) Liu et al 2010 (10) Rautenberger et al 2015 (12) Cornwall et al 2012 (13) Surif and Raven 1993, (14) Ni'Longphui et al 2013, (15) Zou and Gao 2010 (16) Russel et al 2009, (17) Zou et al 2011 (19) Fernandez et al 2014 (18) Enríquez and Rodríguez- Román 2006 (21) Nunes et al 2016 (22) Anthony et al 2008 (23) Mercado 1999 (24) Cornwall et al 2014 (25) Noisette et al 2013 (26) Gao et al 1991 (27) Gao and Zheng 2010 (28) Semesi et al 2009 (29) Hoffman et al 2012

Table 2.1. Average net photosynthesis maxima (P_{\max} $\mu\text{mol O}_2 \text{ g}^{-1} \text{ min}^{-1}$), gross photosynthesis maxima (P_{gmax} $\mu\text{mol O}_2 \text{ g}^{-1} \text{ min}^{-1}$), photosynthetic efficiency (α $\mu\text{mol O}_2 / \mu\text{mol photons}$), respiration (R $\mu\text{mol O}_2 \text{ g}^{-1} \text{ min}^{-1}$) and light compensation point (I_c $\mu\text{mol photons m}^{-2} \text{ s}^{-1}$) for *L. variegata* and *Peyssonnelia sp.* at pH 7.5, 7.8, 8.1, and 8.5, corresponding to 99, 349, 805, 1740 ppm $p\text{CO}_2$. Photosynthetic parameters were calculated using the hyperbolic tangent equation (Jassby and Platt 1976).

Treatment	P_{\max}	P_{gmax}	α	R	I_c
<i>L. variegata</i>					
7.5	0.84 ± 0.10^a	1.30 ± 0.18^a	$1.0\text{E-}2 \pm 2.8\text{E-}3$	0.46 ± 0.12	55 ± 10
7.8	$0.56 \pm 0.06^{a,b}$	0.85 ± 0.05^{ab}	$0.6\text{E-}2 \pm 1.6\text{E-}3$	0.29 ± 0.05	68 ± 23
8.1	$0.41 \pm 0.08^{b,c}$	0.68 ± 0.07^{bc}	$0.9\text{E-}2 \pm 3.7\text{E-}3$	0.27 ± 0.04	51 ± 15
8.5	0.17 ± 0.04^c	0.50 ± 0.04^c	$0.7\text{E-}2 \pm 2.1\text{E-}3$	0.33 ± 0.06	93 ± 33
<i>Peyssonnelia sp.</i>					
7.5	0.05 ± 0.02	0.11 ± 0.02	$1.4\text{E-}3 \pm 1.3\text{E-}4$	0.06 ± 0.01	97 ± 40
7.8	0.06 ± 0.02	0.15 ± 0.02	$1.1\text{E-}3 \pm 1.3\text{E-}4$	0.09 ± 0.01	155 ± 33
8.1	0.05 ± 0.02	0.10 ± 0.03	$0.2\text{E-}3 \pm 7.8\text{E-}5$	0.05 ± 0.01	98 ± 24
8.5	0.02 ± 0.02	0.08 ± 0.03	$0.4\text{E-}3 \pm 1.0\text{E-}4$	0.06 ± 0.01	164 ± 18

Table 2.2. One-Way ANOVA results on net photosynthesis maxima (P_{\max}), gross photosynthesis maxima ($P_{g\max}$), photosynthetic efficiency (α), respiration (R) and light compensation point (I_c) in response to pH for *L. variegata* and *Peyssonnelia sp.*

Significant effects ($p < 0.5$) are marked with an asterisk.

Parameter	df	Sum Sq	Mean Sq	F value	<i>p</i> -value
<i>L. variegata</i>					
P_{\max}	3	1.4139	0.4713	14.27	3.34e-05 *
$P_{g\max}$	3	0.6655	0.22185	10.95	1.81e-4 *
α	3	1.716e-05	5.719e-06	0.547	0.656
R	3	0.01096	0.003653	1.288	0.306
I_c	3	0.2106	0.07021	0.814	0.501
<i>Peyssonnelia sp.</i>					
P_{\max}	3	0.001799	0.0005995	1.018	0.419
$P_{g\max}$	3	0.008083	0.002694	1.275	0.327
α	3	0.000437	0.0001457	0.797	0.519
R	3	0.003388	0.001129	0.856	0.49
I_c	3	10262	3421	0.728	0.557

Table 2.3. Average (\pm SE) net maximum photosynthesis (P_{\max} $\mu\text{mol O}_2 \text{ g}^{-1} \text{ min}^{-1}$), gross maximum photosynthesis (P_{gmax} $\mu\text{mol O}_2 \text{ g}^{-1} \text{ min}^{-1}$), photosynthetic efficiency (α $\mu\text{mol O}_2 / \mu\text{mol photons}$), respiration (R $\mu\text{mol O}_2 \text{ g}^{-1} \text{ min}^{-1}$) and light compensation point (I_c $\mu\text{mol photons m}^{-2} \text{ s}^{-1}$) for *Lobophora variegata* and *Peyssonnelia sp.* of a control and in the presence of four inhibitors. Inhibitors with significant effect ($p < 0.5$) are marked with an asterisk. Parameters are calculated using the hyperbolic tangent equation (Jassby and Platt 1976).

Inhibitors	P_{\max}	P_{gmax}	α	R	I_c
<i>L. variegata</i>					
Control	0.41 \pm 0.08	0.68 \pm 0.07	9.1E-3 \pm 3.7E-3	0.27 \pm 0.04	52 \pm 15
AZ	0.18 \pm 0.04*	0.55 \pm 0.08	9.4E-3 \pm 2.8E-3	0.37 \pm 0.07	77 \pm 23
PLP	0.29 \pm 0.08	0.52 \pm 0.07	4.2E-3 \pm 7.5E-4	0.23 \pm 0.05	125 \pm 79
Van	0.28 \pm 0.05	0.60 \pm 0.07	7.2E-3 \pm 1.6E-3	0.32 \pm 0.04	63 \pm 9
Tris	0.46 \pm 0.04	0.82 \pm 0.08	5.7E-3 \pm 9.6E-4	0.36 \pm 0.06	76 \pm 12
<i>Peyssonnelia sp.</i>					
Control	0.05 \pm 0.01	0.11 \pm 0.01	0.6E-3 \pm 9.8E-5	0.06 \pm 0.01	136 \pm 26
AZ	0.02 \pm 0.00*	0.10 \pm 0.02	1.4E-3 \pm 5.0E-4	0.08 \pm 0.02	111 \pm 23
PLP	0.01 \pm 0.01*	0.07 \pm 0.01	0.6E-3 \pm 2.6E-4	0.06 \pm 0.01	261 \pm 70
Van	0.03 \pm 0.01	0.08 \pm 0.01	0.4E-3 \pm 4.2E-5	0.05 \pm 0.01	268 \pm 140
Tris	0.02 \pm 0.01*	0.10 \pm 0.01	0.9E-3 \pm 1.4E-4	0.08 \pm 0.01	144 \pm 35

Table 2.4. One-Way ANOVA results for inhibitors effects on net photosynthesis maxima (P_{\max}), gross photosynthesis maxima ($P_{g\max}$), photosynthetic efficiency (α), respiration (R) and light compensation point (I_c) for *Lobophora variegata* and *Peyssonnelia sp.* Results for α for *Peyssonnelia* did not meet assumptions of normality of residuals and homogeneity of variances and so a non-parametric Kruskal-Wallis test was used. Significant effects ($p < 0.5$) are marked with an asterisk.

	df	Sum Sq	Mean Sq	F value	p-value
<i>L. variegata</i>					
P_{\max}	4	3.019E-1	7.548 E-2	3.718	0.0166*
$P_{g\max}$	4	3.557E-1	8.892 E-2	2.635	0.0579
α	4	1.716E-5	5.719 E-6	0.547	0.656
R	4	8.79 E-3	2.198 E-3	1.247	0.317
I_c	4	1.865 E-1	4.661 E-2	0.387	0.816
<i>Peyssonnelia sp.</i>					
P_{\max}	4	6.227 E-3	1.5568 E-3	3.978	0.0129*
$P_{g\max}$	4	8.168 E-3	2.0421 E-3	2.401	0.078
α	4	-	-	-	0.08751
R	4	1.012 E-3	2.530 E-4	2.428	0.0755
I_c	4	3.193 E-3	7.982 E-2	0.902	0.48

Table 2.5. Average (\pm SE) net primary (NPP) and gross (GPP) productivity and respiration (R) for *Lobophora variegata*, *Dictyota pulchella*, *Halimeda gorreuii*, *Halimeda copiosa*, *Halimeda opuntia*, and *Halimeda tuna* ($\mu\text{g O}_2 \text{ min}^{-1} \text{ g dw}^{-1}$) at pH 7.8, 8.1, and 8.5.

	pH	NPP	R	GPP
<i>L. variegata</i> *	7.8	83 ± 5^a	-38 ± 2	120 ± 7^a
	8.1	53 ± 5^b	-33 ± 2	86 ± 7^b
	8.5	51 ± 4^b	-36 ± 2	87 ± 6^b
<i>D. pulchella</i>	7.8	185 ± 13	-102 ± 7	287 ± 20
	8.1	216 ± 34	-137 ± 18	353 ± 52
	8.5	183 ± 9	-125 ± 9	308 ± 17
<i>H. gorreuii</i> *	7.8	48 ± 9^a	-17 ± 3^a	65 ± 12^a
	8.1	36 ± 5^{ab}	-11 ± 2^{ab}	47 ± 7^{ab}
	8.5	22 ± 5^b	-7 ± 2^b	29 ± 7^b
<i>H. copiosa</i>	7.8	15 ± 3	-5 ± 1	20 ± 3
	8.1	15 ± 3	-5 ± 1	20 ± 4
	8.5	11 ± 3	-5 ± 1	16 ± 4
<i>H. opuntia</i> *	7.8	99 ± 12^a	-49 ± 6	148 ± 18^a
	8.1	85 ± 5^{ab}	-44 ± 5	129 ± 9^{ab}
	8.5	62 ± 9^b	-33 ± 4	95 ± 12^b
<i>H. tuna</i>	7.8	168 ± 16	-58 ± 8	226 ± 22
	8.1	140 ± 21	-57 ± 7	197 ± 29
	8.5	139 ± 15	-45 ± 4	185 ± 18

Table 2.6. One-Way ANOVA results on net productivity (NPP), gross productivity (GPP), and respiration (R) response to pH for *Lobophora variegata*, *Dictyota pulchella*, *Halimeda gorreuii*, *Halimeda copiosa*, *Halimeda opuntia*, and *Halimeda tuna*.

Significant effects ($p < 0.5$) are marked with an asterisk.

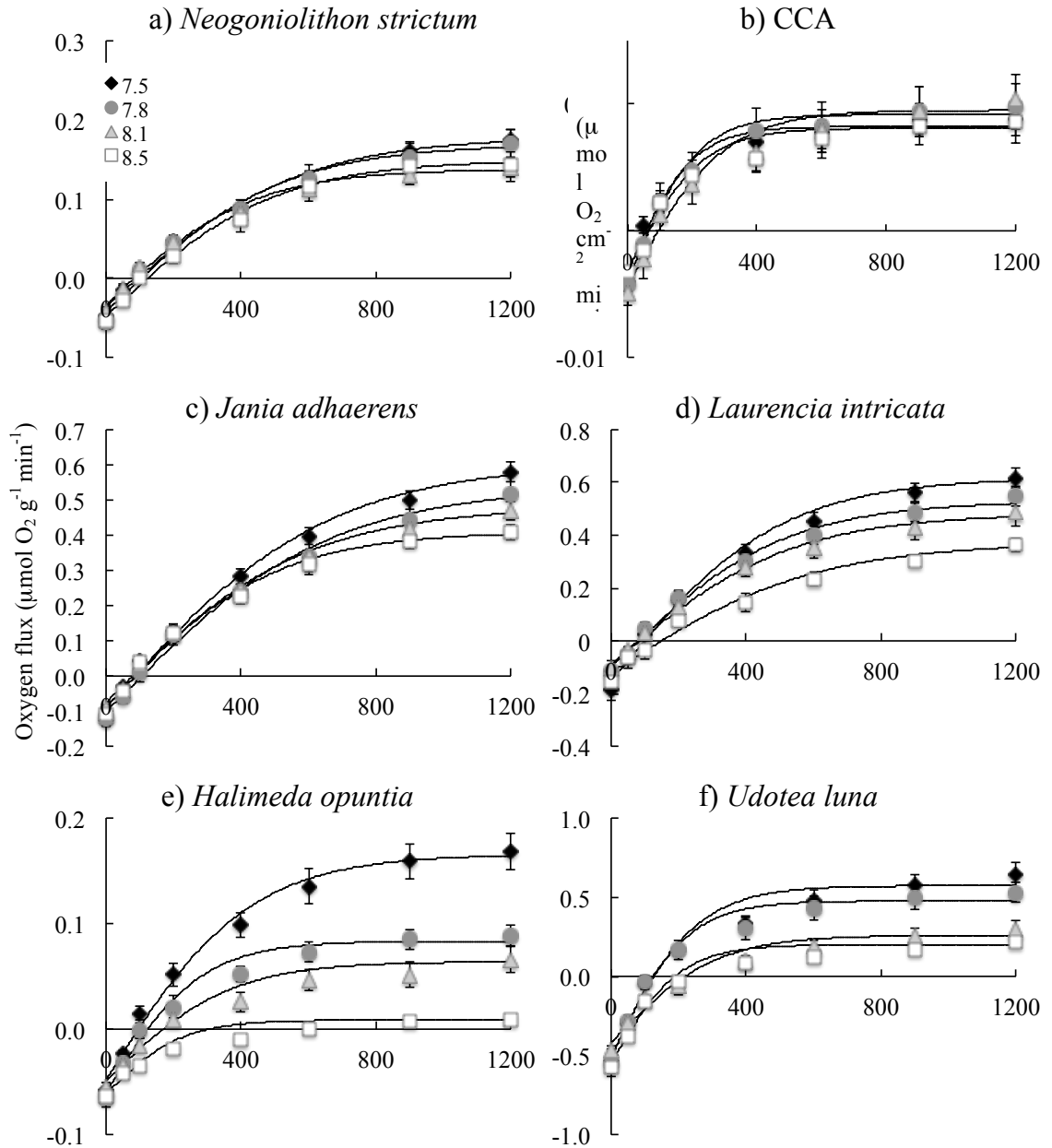
Species	Parameter	df	Sum Sq	Mean Sq	F-value	<i>p</i> -value
<i>L. variegata</i>	NPP	2	6195	3097.5	13.47	8.75e-05 *
	R	2	134	67.01	1.552	0.23
	GPP	2	7711	3855	8.9	0.00107 *
<i>D. pulchella</i>	NPP	2	10629	5315	1.015	0.376
	R	2	10135	5067	2.906	0.072
	GPP	2	38724	19362	1.528	0.235
<i>H. gorreuii</i>	NPP	2	1.161	0.5805	4.007	0.0299 *
	R	2	0.7757	0.3879	6.423	0.00523 *
	GPP	2	0.9135	0.4567	4.763	0.0169 *
<i>H. copiosa</i>	NPP	2	0.1725	0.08623	1.133	0.337
	R	2	0.0269	0.01345	0.254	0.777
	GPP	2	0.1173	0.05867	0.891	0.422
<i>H. opuntia</i>	NPP	2	0.2322	0.11609	4.68	0.018 *
	R	2	1368	684.1	2.676	0.087
	GPP	2	0.2097	0.1049	4.162	0.0266 *
<i>H. tuna</i>	NPP	2	5302	2651	0.866	0.432
	R	2	0.0560	0.02801	1.083	0.353
	GPP	2	8864	4432	0.807	0.456

Appendix 2 – Figures

Figure 1.1 Map of study site in Florida Keys



Fig. 1.2. Photosynthesis–Irradiance (P:I) curves for all species at the four pH levels examined (means (\pm SE of 4-8). P:I curves were fit to a hyperbolic tangent curve (Jassby and Platt 1976) from which photosynthetic parameters were calculated (see Table 1).



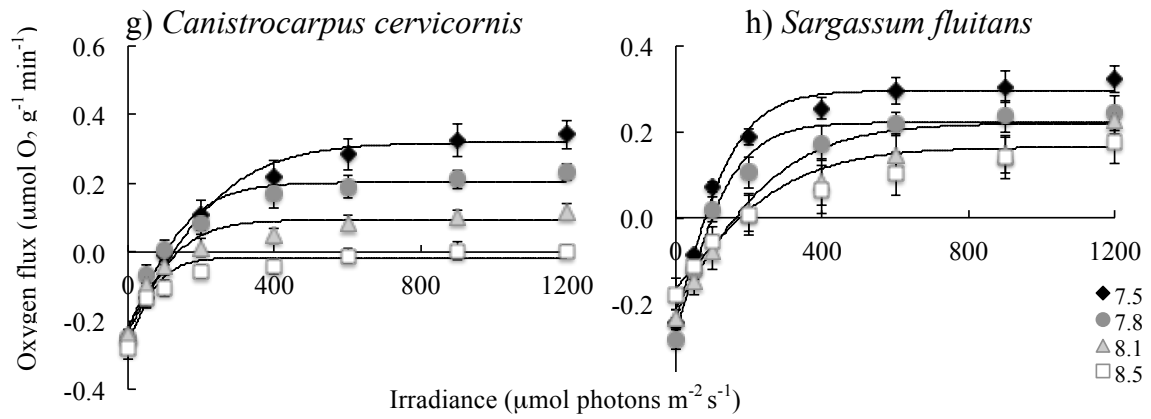
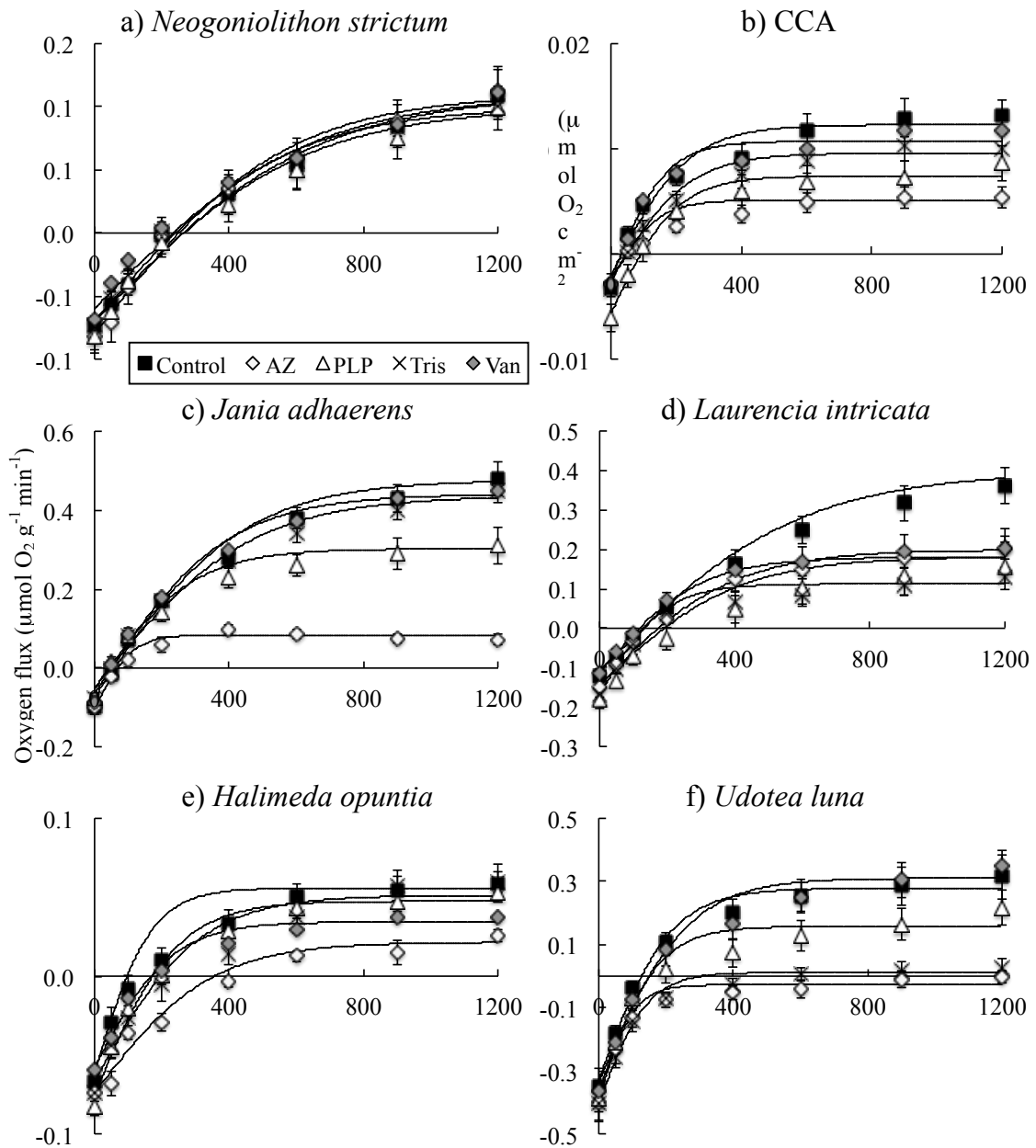


Fig. 1.3. Photosynthesis–Irradiance (P:I) curves of all species exposed to the four inhibitors (see text details): AZ (white diamond), PLP (white triangle), Van (gray diamond), and Tris (black x); and a control (black square). Data are means with SE (n = 8). P:I curves were fit to a hyperbolic tangent curve (Jassby and Platt 1976) from which photosynthetic parameters were calculated (Table 3).



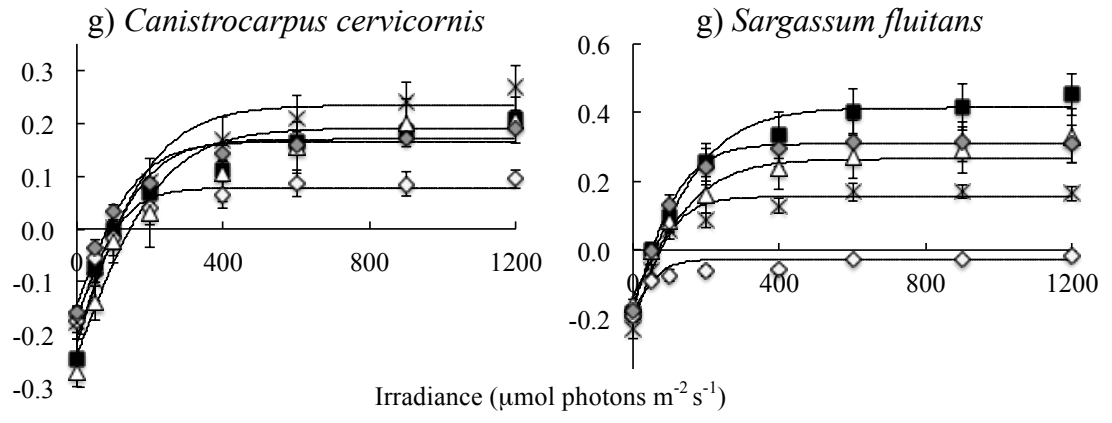


Fig. 1.4. Average gross maximum photosynthesis in response to four pH levels and AZ inhibitor (blocking external carbonic anhydrase). Data are means with SE (n=7 – 8). P:I curves were fit to a hyperbolic tangent curve (Jassby and Platt 1976) from which gross maximum photosynthesis was calculated.

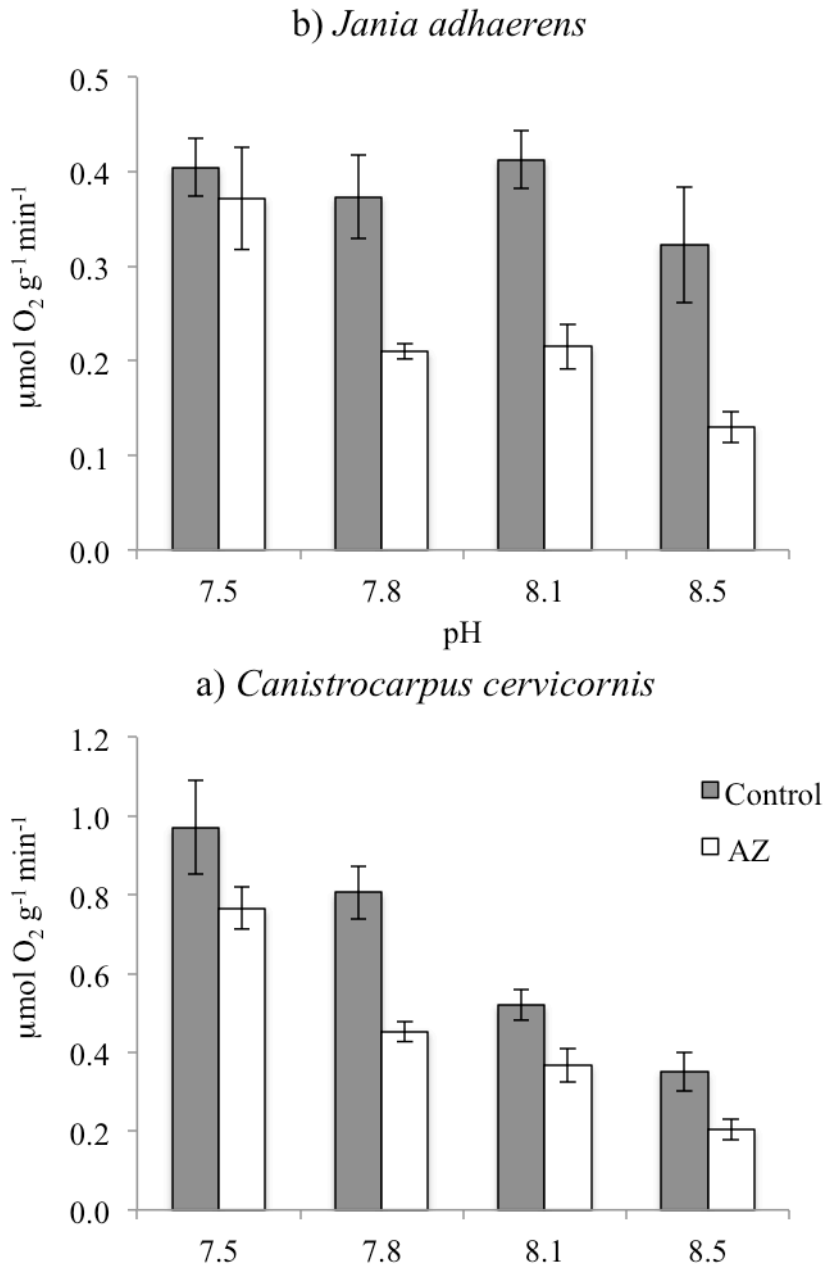


Fig. 1.5. $\delta^{13}\text{C}$ isotope signatures of *Halimeda opuntia* (*H. opu*), *Canistrocarpus cervicornis* (*C. cer*), *Laurencia intricata* (*L. int*), *Jania adhaerens* (*J. adh*), *Sargassum fluitans* (*S. flu*), *Neogoniolithon strictum* (*N. str*) CCA, and *Udotea luna* (*U. lun*).

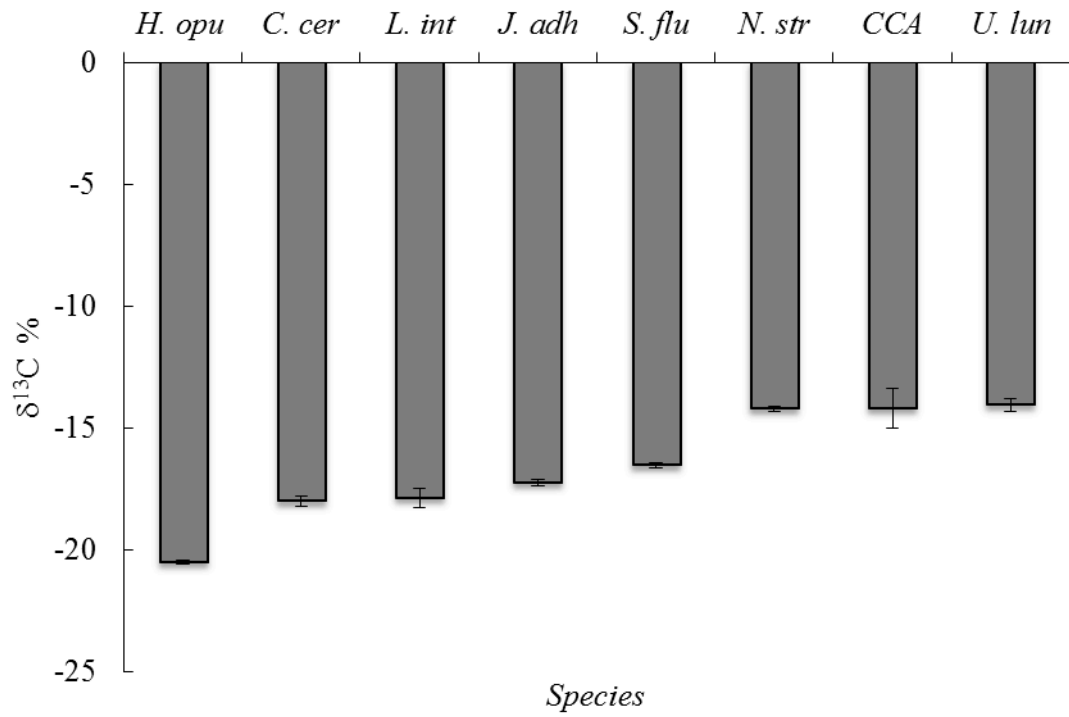


Fig. 2.1. The upper panel shows the location of (A) the Little Cayman Research Centre (LCRC) on the northern coast of Little Cayman Island where experiments were conducted. The two collection sites are also identified, Icon Reef (B) a spur and groove fore-reef (~15 m) ~700 m northeast of LCRC and Rock Bottom (C) an outer fore-reef ledge (~18 m) ~900 m northeast of LCRC. The photos were taken at shallow (upper) and deep (lower) sites on the reef illustrating the high abundance of *Lobophora variegata* (L. var) in both deep and shallow reefs. In the deep reef images, lobed red crustose coralline algae, primarily *Peyssonnelia* sp. (P. sp) can also be seen co-occurring with *Lobophora*. Two *Halimeda* species are also visible *H. gorraeuii* (H. gor) and *H. copiosa* (H. cop) which are major carbonate producers on the reef, seen as white flocculent material on the benthos.

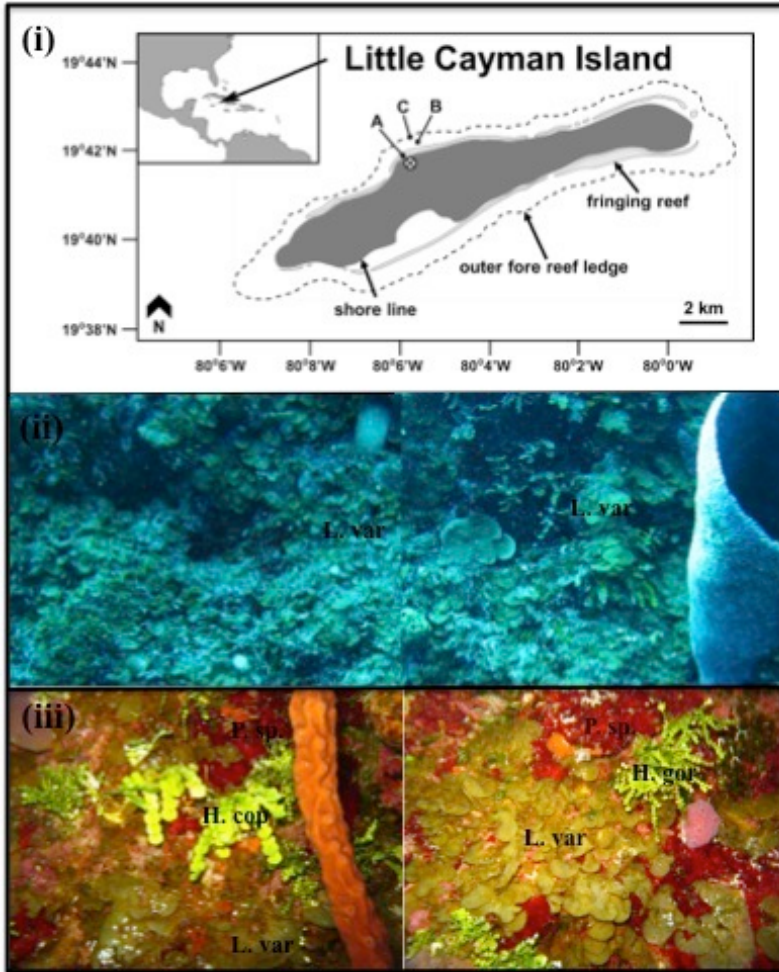


Fig. 2.2. Photosynthesis–Irradiance (P:I) curves for a) *Lobophora variegata* and b) *Peyssonnelia sp.* at 4 pH levels. Data are means +/- SE of 6 replicates for *L. variegata* and 4 replicates for *Peyssonnelia sp.*; individual, independent replicates were used for each pH level. P:I curves were fit to a hyperbolic tangent curve (Jassby and Platt 1976) from which photosynthetic parameters were calculated.

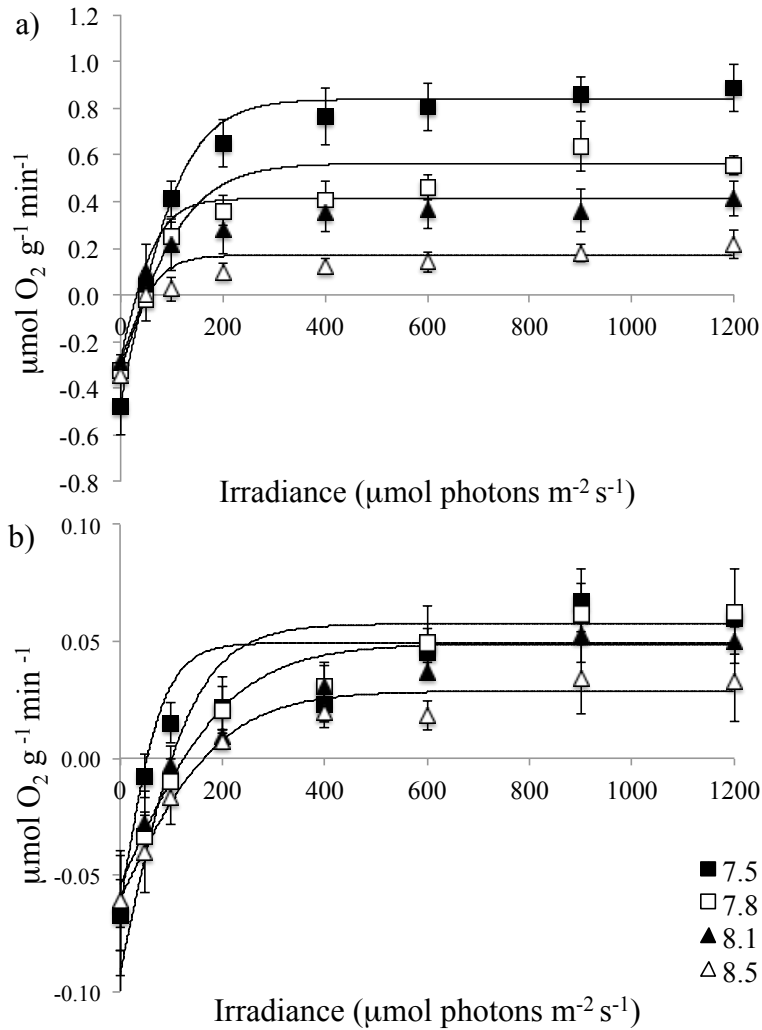
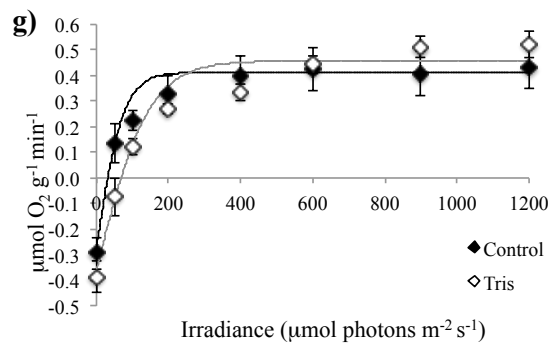
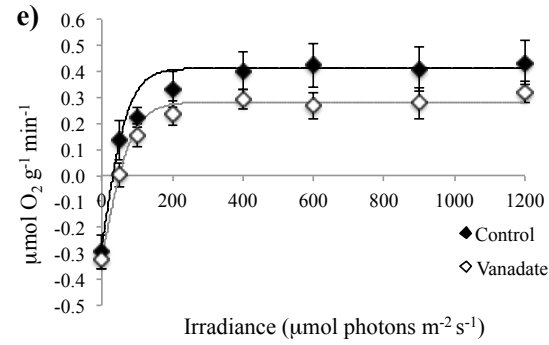
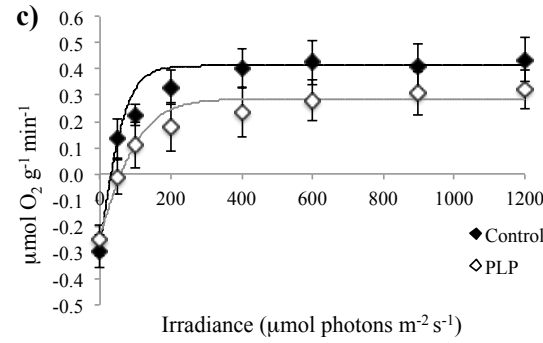
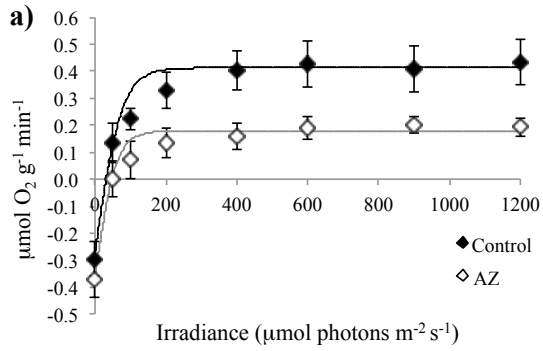


Fig. 2.3. Photosynthesis–Irradiance (P:I) curves for *Lobophora variegata* (a,c,e,g) and *Peyssonnelia sp.* (b,d,f,g) without (control black square) and with inhibitors: AZ (a-b), PLP (c-d), Van (e-f), and Tris (g-h); see text for details on inhibitors. Data are means with SE of n=4-7. P:I curves were fit to a hyperbolic tangent curve (Jassby and Platt 1976) from which photosynthetic parameters were calculated (Table 3).

Lobophora variegata



Peysonnella sp.

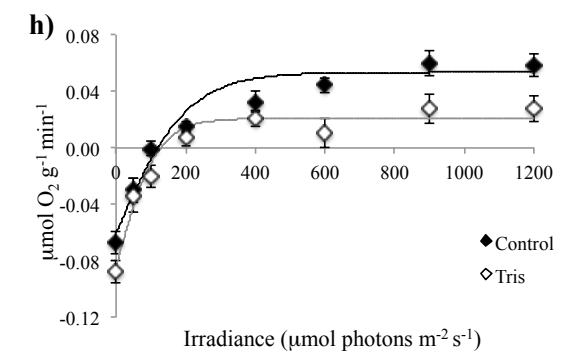
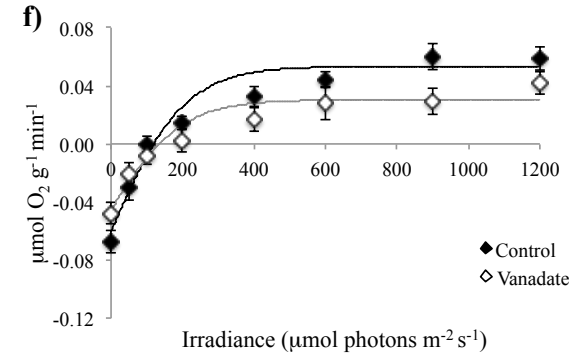
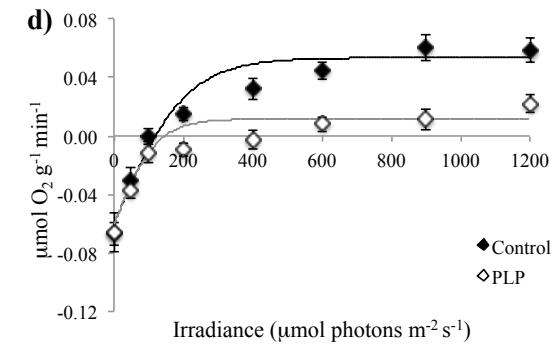
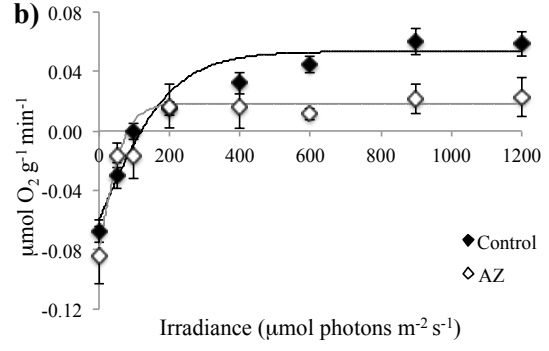
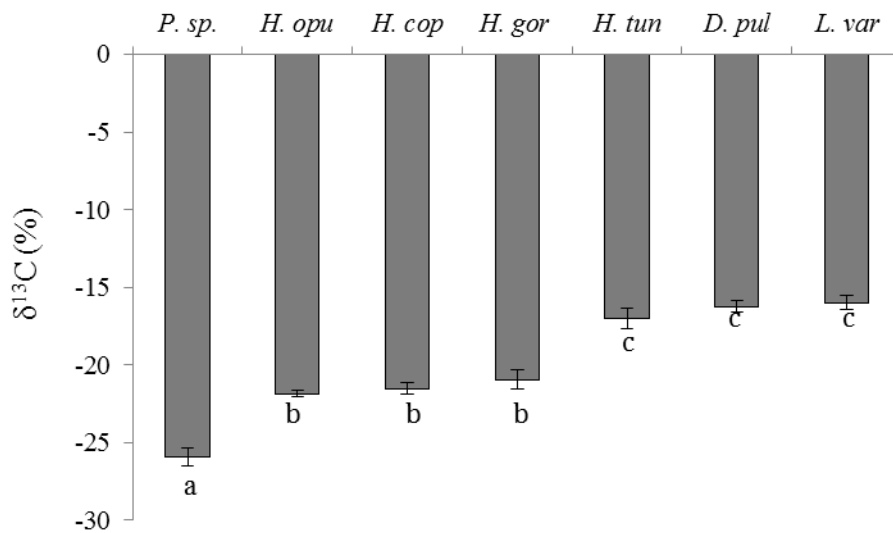


Fig. 2.4. $\delta^{13}\text{C}$ isotope signatures for *Peyssonnelia sp.* (*P. sp.*), *Halimeda opuntia* (*H. opu*), *Halimeda copiosa* (*H. cop*), *Halimeda gorreuii* (*H. gor*), *Halimeda tuna* (*H. tun*), *Lobophora variegata* (*L. var*), and *Dictyota pulchella* (*D. sp*) Differences in species were found to be significant with a One Way ANOVA ($p < 0.05$). Groups with different letters are statistically different (Tukey Pairwise Comparison Test).



References

- Al-Moghrabi S, Goiran C, Allemand D, Speziale N, Jaubert J (1996) Inorganic carbon uptake for photosynthesis by the symbiotic coral - dinoflagellate association II. Mechanisms for bicarbonate uptake. *J Exp Mar Bio Ecol* 199:227–248 .
- Andersson AJ, MacKenzie FT (2012) Revisiting four scientific debates in ocean acidification research. *Biogeosciences* 9:893–905.
- Anthony KRN, Kline DI, Diaz-Pulido G, Dove S, Hoegh-Guldberg O (2008) Ocean acidification causes bleaching and productivity loss in coral reef builders. *Proc Natl Acad Sci* 105:17442–17446.
- Caldeira K, Wickett ME (2003) Oceanography: anthropogenic carbon and ocean pH. *Nature* 425:365 .
- Celis-Plá PS, Hall-spencer JM, Horta PA, Milazzo M, Korbee N, Cornwall CE, Figueroa FL (2015) Macroalgal responses to ocean acidification depend on nutrient and light levels. *Front Mar Sci* 2:1–12.
- Comeau S, Carpenter RC, Edmunds PJ (2016) Effects of $p\text{CO}_2$ on photosynthesis and respiration of tropical scleractinian corals and calcified algae. *ICES J Mar Sci* 73:250–262.
- Cornwall CE, Boyd PW, McGraw CM, Hepburn CD, Pilditch CA, Morris JN, Smith AM, Hurd CL (2014) Diffusion boundary layers ameliorate the negative effects of ocean acidification on the temperate coralline macroalga *Arthrocardia corymbosa*.. *PLoS One* 9:1–9.
- Cornwall CE, Hepburn CD, McGraw CM, Currie KI, Pilditch CA, Hunter KA, Boyd PW, Hurd CL (2013) Diurnal fluctuations in seawater pH influence the response of a calcifying macroalga to ocean acidification. *Proc R Soc* 280:20132201.
- Cornwall CE, Revill AT, Hurd CL (2015) High prevalence of diffusive uptake of CO_2 by macroalgae in a temperate subtidal ecosystem.. *Photosynth Res* 124:181–190.
- Cornwall CE, Hepburn CD, Pritchard D, Currie KI, McGraw CM, Hunter K a., Hurd CL (2012) Carbon-use strategies in macroalgae: differential responses to lowered pH and implications for ocean acidification.. *Phycol Soc Am* 48:137–144.

- Del Monaco C, Hay ME, Gartrell P, Mumby PJ, Diaz-Pulido G (2017) Effects of ocean acidification on the potency of macroalgal allelopathy to a common coral. *Sci Rep* 7:41053.
- Diaz-Pulido G, Cornwall C, Gartrell P, Hurd C, Tran D V. (2016) Strategies of dissolved inorganic carbon use in macroalgae across a gradient of terrestrial influence: implications for the Great Barrier Reef in the context of ocean acidification. *Coral Reefs* 35:1327–1341.
- Diaz-Pulido G, Gouezo M, Tilbrook B, Dove S, Anthony KRN (2011) High CO₂ enhances the competitive strength of seaweeds over corals. *Ecol Lett* 14:156–62.
- Doney SC, Fabry VJ, Feely R a, Kleypas J a (2009) Ocean acidification: the other CO₂ problem. *Ann Rev Mar Sci.* 1:169–92.
- Drechsler Z, Sharkia R, Cabantchik I, Beer S (1993) Bicarbonate uptake in marine macroalga *Ulva sp.* is inhibited by classical probes of anion exchange by red blood cells. *Planta* 191:34–40.
- Dutra E, Koch M, Peach K, Manfrino C (2016) Tropical crustose coralline algal individual and community responses to elevated *p*CO₂ under high and low irradiance. *ICES J Mar Sci* 73:803–813.
- Edmunds PJ (2002) Long-term dynamics of coral reefs in St . John, US Virgin Islands. *Coral Reefs.* 21:357–367.
- Enochs IC, Manzello DP, Donham EM, Kolodziej G, Okano R, Johnston L, Young C, Iguel J, Edwards CB, Fox MD, Valentino L, Johnson S, Benavente D, Clark SJ, Carlton R, Burton T, Eynaud Y, Price NN (2015) Shift from coral to macroalgae dominance on a volcanically acidified reef. *Nat Clim Chang* 5:1–9.
- Enríquez S, Rodríguez-Román a (2006) Effect of water flow on the photosynthesis of three marine macrophytes from a fringing-reef lagoon. *Mar Ecol Prog Ser* 323:119–132.
- Fabricius KE, Langdon C, Uthicke S, Humphrey C, Noonan S, De 'ath G, Okazaki R, Muehllehner N, Glas MS, Lough JM (2011) Losers and winners in coral reefs acclimatized to elevated carbon dioxide concentrations. *Nat Clim Chang* 1:165–169.
- Feely R a, Sabine CL, Lee K, Berelson W, Kleypas J, Fabry VJ, Millero FJ (2004) Impact of anthropogenic CO₂ on the CaCO₃ system in the oceans. *Science* 305:362–6.
- Fernández P A, Hurd CL, Roleda MY (2014) Bicarbonate uptake via an anion exchange protein is the main mechanism of inorganic carbon acquisition by the giant kelp

- Macrocystis pyrifera* (Laminariales, Phaeophyceae) under variable pH.. J Phycol 50:998–1008.
- Fong P, Paul VJ (2011) Coral Reefs: An Ecosystem in Transition. In: Dubinsky Z., Stambler N. (eds) Springer Netherlands, Dordrecht, pp 241–272.
- Gao K, Aruga Y, Asada K, Ishihara T, Akano T, Kiyohara M (1991) Enhanced growth of the red alga *Porphyra yezoensis* Ueda in high CO₂ concentrations. J Appl Phycol 3:355–362.
- Gao K, Zheng Y (2010) Combined effects of ocean acidification and solar UV radiation on photosynthesis, growth, pigmentation and calcification of the coralline alga *Corallina sessilis* (Rhodophyta). Glob Chang Biol 16:2388–2398.
- Giordano M, Beardall J, Raven J a (2005) CO₂ concentrating mechanisms in algae: mechanisms, environmental modulation, and evolution. Annu Rev Plant Biol 56:99–131.
- Hall-Spencer JM, Rodolfo-Metalpa R, Martin S, Ransome E, Fine M, Turner SM, Rowley SJ, Tedesco D, Buia MC (2008) Volcanic carbon dioxide vents show ecosystem effects of ocean acidification. Nature 454:96–99.
- Haglund K, Björk M, Ramazanov Z, García-Reina G, Pedersén M (1992) Role of carbonic anhydrase in photosynthesis and inorganic-carbon assimilation in the red alga *Gracilaria tenuistipitata*. Planta 187:275–281.
- Hepburn CD, Pritchard DW, Cornwall CE, McLeod RJ, Beardall J, Raven JA, Hurd CA (2011) Diversity of carbon use strategies in a kelp forest community: implications for a high CO₂ ocean. Glob Chang Biol 17:2488–2497.
- Heyward AJ, Negri AP (1999) Natural inducers for coral larval metamorphosis. Coral Reefs 18:273–279.
- Hillis LW (1997) Corallgal reefs from a calcareous green alga perspective, and a first carbonate budget. In: Proc 8th Int Coral Reef Sym, Panama City, p 761–766.
- Hofmann GE, Smith JE, Johnson KS, Send U, Levin LA, Micheli F, Paytan A, Price NN, Peterson B, Takeshita Y, Matson PG, de Crook E, Kroeker KJ, Gambi MC, Rivest EB, Frieder CA, Yu PC, Martz TR (2011) High-frequency dynamics of ocean pH: A multi-ecosystem comparison. PLoS One 6: e28983.
- Hofmann LC, Yildiz G, Hanelt D, Bischof K (2012) Physiological responses of the calcifying rhodophyte , *Corallina officinalis* (L .), to future CO₂ levels. 783–792

- Hofmann LC, Fink A, Bischof K, de Beer D (2015) Microsensor studies on *Padina* from a natural CO₂ seep: Implications of morphology on acclimation to low pH. *J Phycol* 51:1106–1115.
- Hofmann LC, Heiden J, Bischof K, Teichberg M (2014) Nutrient availability affects the response of the calcifying chlorophyte *Halimeda opuntia* (L.) J.V. Lamouroux to low pH. *Planta* 239:231–242.
- Hughes TP (1994) Catastrophes, phase-shifts and large-scale degradation of a Caribbean coral reef. *Science* 265:1547–1551.
- Hughes TP, Graham NAJ, Jackson JBC, Mumby PJ, Steneck RS (2010) Rising to the challenge of sustaining coral reef resilience. *Trends Ecol Evol* 25:633–642.
- Hurd CL, Hepburn CD, Currie KI, Raven JA, Hunter KA (2009) Testing the effects of ocean acidification on algal metabolism: considerations for experimental designs. *J Phycol* 45:1236–51.
- Hurd CL, Cornwall CE, Currie K, Hepburn CD, McGraw CM, Hunter K a., Boyd PW (2011) Metabolically induced pH fluctuations by some coastal calcifiers exceed projected 22nd century ocean acidification: a mechanism for differential susceptibility? *Glob Chang Biol* 17:3254–3262.
- IPCC (Intergovernmental Panel on Climate Change) (2013) *Climate change 2013: The physical science basis. Contribution of Working Group I to the Fifth Assessment Report of the Intergovernmental Panel on Climate Change.* Cambridge University Press, Cambridge.
- Israel A, Hophy M (2002) Growth, photosynthetic properties and Rubisco activities and amounts of marine macroalgae grown under current and elevated seawater CO₂ concentrations. *Glob Chang Biol* 2:831–840.
- James RK, Hepburn CD, Cornwall CE, McGraw CM, Hurd CL (2014) Growth response of an early successional assemblage of coralline algae and benthic diatoms to ocean acidification. *Mar Biol* 161:1687–1696.
- Jassby AD, Platt T (1976) Mathematical formulation of the relationship between photosynthesis and light for phytoplankton. *Limnol Oceanogr* 21: 540–547.
- Ji Y, Xu Z, Zou D, Gao K (2016) Ecophysiological responses of marine macroalgae to climate change factors. *J Appl Phycol* 2953–2967.
- Johnson MD, Price NN, Smith JE (2014) Contrasting effects of ocean acidification on tropical fleshy and calcareous algae. *PeerJ* 2:e411.

- Klenell M, Snoeijs P, Pedersén M (2002) The involvement of a plasma membrane H⁺-ATPase in the blue-light enhancement of photosynthesis in *Laminaria digitata* (Phaeophyta). *J Phycol* 38:1143–1149.
- Koch M, Bowes G, Ross C, Zhang X-H (2013) Climate change and ocean acidification effects on seagrasses and marine macroalgae. *Glob Chang Biol* 19:103–32.
- Kroeker KJ, Gambi MC, Micheli F (2013) Community dynamics and ecosystem simplification in a high-CO₂ ocean. *Proc Natl Acad Sci U S A* 110:12721–6.
- Kroeker KJ, Kordas RL, Crim RN, Singh GG (2010) Meta-analysis reveals negative yet variable effects of ocean acidification on marine organisms. *Ecol Lett* 13:1419–34.
- Kroeker KJ, Kordas RL, Crim R, Hendriks IE, Ramajo L, Singh GS, Duarte CM, Gattuso JP (2013) Impacts of ocean acidification on marine organisms: Quantifying sensitivities and interaction with warming. *Glob Chang Biol* 19:1884–1896.
- Kübler JE, Johnston AM, Raven JA (1999) The effects of reduced and elevated CO₂ and O₂ on the seaweed *Lomentaria articulata*. *Plant Cell Environ* 22:1303–1310.
- Kübler JE, Dudgeon SR (2015) Predicting effects of ocean acidification and warming on algae lacking carbon concentrating mechanisms. *PLoS One* 10:1–19 .
- Kuffner IB, Andersson AJ, Jokiel PL, Rodgers KS, Mackenzie FT (2008) Decreased abundance of crustose coralline algae due to ocean acidification. *Nat Geosci* 1: 114–117.
- Larsson C, Axelsson L (1999) Bicarbonate uptake and utilization in marine macroalgae. *Eur J Phycol* 34:79–86.
- Larsson C, Axelsson L, Ryberg H, Beer S (1997) Photosynthetic carbon utilization by *Enteromorpha intestinalis* (Chlorophyta) from a Swedish rockpool. *Eur J Phycol* 32:49–54.
- Lobo FA, Barros MP, Dalmagro HJ, Dalmolin ÂC (2013) Fitting net photosynthetic light-response curves with Microsoft Excel — a critical look at the models. *Photosynthetica* 51: 445–456.
- Liddell WD, Ohlhorst SL (1986) Changes in benthic community composition following the mass mortality of *Diadema* at Jamaica. *J Exp Mar Bio Ecol* 95:271–278.
- Liu Y, Xu J, Gao K (2012) CO₂ -driven seawater acidification increases photochemical stress in a green alga. *Phycologia* 51:562–566.
- Maberly SC, Raven JA, Johnston AM (1992) Discrimination between ¹²C and ¹³C by marine plants. *Oecologia* 91:481–492.

- Mercado JM, Andría JR, Pérez-Llorens JL, Vergara JJ, Axelsson L (2006) Evidence for a plasmalemma-based CO₂ concentrating mechanism in *Laminaria saccharina*. *Photosynth Res* 88:259–68.
- Mercado JM, Figueroa F, Xauier Niell F, Axelsson L (1997) A new method for estimating external, carbonic anhydrase activity in macroalgae. *J Phycol* 33:999–1006.
- Mercado JM, Javier F, Gordillo L, Niell FX, Figueroa L (1999) Effects of different levels of CO₂ on photosynthesis and cell components of the red alga *Porphyra leucosticta*. *J Appl Phycol* 11:455–461.
- Moulin P, Andría JR, Axelsson L, Mercado JM (2011) Different mechanisms of inorganic carbon acquisition in red macroalgae (Rhodophyta) revealed by the use of TRIS buffer. *Aquat Bot* 95:31–38.
- Mumby PJ, Foster NL, Fahy EAG (2005) Patch dynamics of coral reef macroalgae under chronic and acute disturbance. *Coral Reefs* 24:681–692.
- Ní Longphuirt S, Eschmann C, Russell C, Stengel D (2013) Seasonal and species-specific response of five brown macroalgae to high atmospheric CO₂. *Mar Ecol Prog Ser* 493:91–102.
- Noisette F, Duong G, Six C, Davoult D, Martin S (2013) Effects of elevated pCO₂ on the metabolism of a temperate rhodolith *Lithothamnion corallioides* grown under different temperatures. *J Phycol* 49:746–757.
- Nunes J, McCoy SJ, Findlay HS, Hopkins FE, Kitidis V, Rayner L, Widdicombe S, Queiro AM (2015) Two intertidal, non-calcifying macroalgae (*Palmaria palmata* and *Saccharina latissima*) show complex and variable responses to short-term CO₂ acidification. *ICES J Mar Sci*.
- Olischläger M, Bartsch I, Gutow L, Wiencke C (2013) Effects of ocean acidification on growth and physiology of *Ulva lactuca* (Chlorophyta) in a rockpool-scenario. *Phycol Res* 61:180–190.
- Peach KE, Koch MS, Blackwelder PL (2016) Effects of elevated pCO₂ and irradiance on growth, photosynthesis and calcification in *Halimeda discoidea*. *Mar Ecol Prog Ser* 544:143–158.
- Peach KE, Koch MS, Blackwelder PL, Manfrino C (2017) Calcification and photophysiology responses to elevated pCO₂ in six *Halimeda* species from contrasting irradiance environments on Little Cayman Island reefs. *J Exp Mar Bio Ecol* 486:114–126.

- Pierrot D, Lewis E, Wallace DWR 2006. MS Excel program developed for CO₂ systems calculations: ORNL/CDIAC 105a. Carbon Dioxide Information Analysis Center, Oak Ridge National Laboratory, US Department of Energy, Oak Ridge, TN.
- Porzio L, Buia MC, Hall-Spencer JM (2011) Effects of ocean acidification on macroalgal communities. *J Exp Mar Bio Ecol* 400:278–287.
- Price NN, Martz TR, Brainard RE, Smith JE (2012) Diel variability in seawater pH relates to calcification and benthic community structure on coral reefs. *PLoS One* 7:e43843.
- Price NN, Hamilton SL, Tootell JS, Smith JE (2011) Species-specific consequences of ocean acidification for the calcareous tropical green algae *Halimeda*. *Mar Ecol Prog Ser* 440:67–78 .
- Raimondi PT, Morse ANC (2000) The consequences of complex larval behavior in a coral. *Ecology* 81:3193–3211.
- Rautenberger R, Fernández P a, Strittmatter M, Heesch S, Cornwall CE, Hurd CL, Roleda MY (2015) Saturating light and not increased carbon dioxide under ocean acidification drives photosynthesis and growth in *Ulva rigida* (Chlorophyta). *Ecol Evol* 5:874–88 .
- Raven JA (1997) Putting the C in phycology. *Raven, J A* 32:319–333.
- Raven JA, Beardall J, Giordano M (2014) Energy costs of carbon dioxide concentrating mechanisms in aquatic organisms. *Photosynth Res* 121:111–124.
- Raven JA, Johnston AM, Kübler JE, Korb R, McNroy SG, Handley LL, Scrimgeour CM, Walker DI (2002) Mechanistic interpretation of carbon isotope discrimination by marine macroalgae and seagrasses. *Funct Plant Biol* 29:335–378.
- Raven JA, Giordano M, Beardall J, Maberly SC (2011) Algal and aquatic plant carbon concentrating mechanisms in relation to environmental change. *Photosynth Res* 109:281–296.
- Russell BD, Thompson JAI, Falkenberg LJ, Connell SD (2009) Synergistic effects of climate change and local stressors: CO₂ and nutrient-driven change in subtidal rocky habitats. *Glob Chang Biol* 15:2153–2162.
- Sangil C, Clemente S, Brito A, Rodríguez A, Balsalobre M, Mendoza JC, Martínez D, Hernández JC (2016) Seaweed community response to a massive CO₂ input. *Estuar Coast Shelf Sci* 178:48–57.

- Semesi IS, Kangwe J, Björk M (2009) Alterations in seawater pH and CO₂ affect calcification and photosynthesis in the tropical coralline alga, *Hydrolithon sp.* (Rhodophyta). *Estuar Coast Shelf Sci* 84:337–341.
- Sinutok, S, Hill, R, Doblin, MA, Wuhrer, R, Ralph, PJ, (2011) Warmer more acidic conditions cause decreased productivity and calcification in subtropical coral reef sediment-dwelling calcifiers. *Limnol. Oceanogr.* 56:1200–1212.
- Strong AL, Kroeker KJ, Teneva LT, Mease LA, Kelly RP (2014) Ocean acidification 2.0: Managing our Changing Coastal Ocean Chemistry. *Bioscience* 64:581–592.
- Surif MB, Raven JA (1989) Exogenous inorganic carbon sources for photosynthesis by members of the Fucales and the Laminariales (Phaeophyta): ecological and taxonomic implications. *Oecologia* 78:97–105.
- Vogel N, Meyer FW, Wild C, Uthicke S (2015) Decreased light availability can amplify negative impacts of ocean acidification on calcifying coral reef organisms. *Mar Ecol Prog Ser* 521:49–61.
- Wootton JT, Pfister C a, Forester JD (2008) Dynamic patterns and ecological impacts of declining ocean pH in a high-resolution multi-year dataset. *Proc Natl Acad Sci U S A* 105:18848–53.
- Zar JH (2010). *Biostatistical Analysis*. Pearson Prentice Hall, Inc., New Jersey.
- Zou D, Gao K (2010) Acquisition of inorganic carbon by *Endarachne binghamiae* (Scytosiphonales, Phaeophyceae). *Eur J Phycol* 45:117–126.
- Zou D, Gao K, Chen W (2011) Photosynthetic carbon acquisition in *Sargassum henslowianum* (Fucales, Phaeophyta), with special reference to the comparison between the vegetative and reproductive tissues. *Photosynth Res* 107:159–68.